Kīlauea's Pu'u 'Ō'ō Eruption (1983-2018): A Synthesis of Magmatic Processes During a Prolonged Basaltic Event

3 4

1

2

Michael O. Garcia*

Department of Earth Sciences, University of Hawai'i, Honolulu, HI, 96822, USA

5 6 7

Aaron J. Pietruszka

Department of Earth Sciences, University of Hawai'i, Honolulu, HI, 96822, USA

8

10 Marc D. Norman

Research School of Earth Sciences, The Australian National University, Canberra ACT 2601,

12 Australia

13 14

J. Michael Rhodes

Department of Geoscience, University of Massachusetts, Amherst, MA 01003, USA

15 16

17 * Corresponding author

18 Email: mogarcia@hawaii.edu

19

20

21

22

23

24

25

26

27

28

29

30

31

32

33

34

35

36

37

38

Keywords: Hawaii, volcano, geochemistry, magma, timeseries

Abstract

Kīlauea's Pu'u 'Ō'ō eruption was the longest lived (35+ years), and most voluminous (~4.4 km³) and intensely monitored historical eruption of this Hawaiian volcano. A synthesis and update are presented here on the remarkable petrologic and geochemical evolution of lava erupted from its inception on 03 Jan. 1983 to its demise on 01 May 2018. This time-series analysis chronicled mantle and crustal processes that varied during this eruption, which had more than a two-fold lava effusion rate increase. Our frequent sampling of Pu'u 'Ō'ō lava allowed the changes in crustal and mantle process during this single magmatic event to be assessed. New major element, trace element, and Sr isotope data are presented here for the period from 2010-2018. These results are combined with our previous geochemical studies to reveal the complex interplay of crustal processes that dominated the eruption's first 500 days. Subsequently, mantle geochemical signatures became discernible as the crustal-stored magma was flushed from the conduit system and replace by new mantle-derived magma. This flushing was possible because of the relatively small size of the summit magma reservoir system compared to the volume of magma erupted at Pu'u 'Ō'ō (≤0.2 vs. 4.4 km³). Parental magma compositions changed rapidly during the eruption reflecting source heterogeneity in the mantle plume. The depth of melt segregation may have also changed during the eruption. These results demonstrate the importance of systematic temporal sampling during an active eruption.

1. Introduction

Kīlauea volcano is a superb venue for understanding basaltic volcanism because of its high eruption frequency, easy access, and unique geological setting in the central Pacific Ocean, 1000's of km from plate boundaries or continents (Garcia, 2015). Studies of Hawaiian volcanoes helped shape our understanding of Earth processes from the deep mantle to the atmosphere (e.g., Poland et al., 2014). Time-series geochemical studies of Hawaiian and other ocean island basalts have documented long-term (thousands of years) geochemical variations from studies of deep (>1 km) drill cores (e.g., Caroff et al., 1995; Albarède, 1996; Albarède et al., 1997; Quane et al., 2000; Blichert-Toft et al., 2003; Bryce et al., 2005; Rhodes et al., 2012) and wellexposed stratigraphic sections (Rhodes et al., 1989; Marske et al., 2007; Weis et al., 2011). These studies chronicle processes on millennium time scales. Unfortunately, a complete time series of a volcano's magmatic history is never preserved in a single stratigraphic section. Short-term variations (months to years) in lava chemistry, where samples have been collected in chronological order, have documented geochemical variations that improved our understanding of the temporal and spatial resolution of melting processes and the chemical structure of mantle plumes and crustal processes (e.g., Hofmann et al., 1984; Albarède and Tamagnan, 1988; Pietruszka and Garcia, 1999; Rhodes and Hart, 1995; Vlastelic et al., 2009).

Kīlauea is one of the most active and best-monitored volcanoes in the world (Tilling and Dvorak, 1993; Garcia, 2015). Among historical Kīlauea eruptions, Pu'u 'Ō'ō was the longest (>35 years) and most voluminous (~4.4 km³). We define this eruption as the events and lava erupted in Kīlauea's east rift zone starting on 03 January 1983 and ending on 01 May 2018 (Fig. 1). We exclude from this analysis the coeval activity that occurred at the summit, where a lava lake was active for 10 years (2008-2018), and the lower east rift eruption in May-August 2018, which followed the end of the middle east rift activity and the collapse of the Pu'u 'Ō'ō eruptive center. The other eruptions are the subject of separate studies because they are geochemically distinct (e.,g., Gansecki et al., 2019; Pietruszka et al., 2021).

The Pu'u 'Ō'ō eruption was intensely monitored in the field, and remotely for earthquakes and ground deformation (e.g., Wolfe et al., 1988; Heliker et al., 2003; Poland et al., 2012; Orr et al., 2015). The long duration and vigorous activity (~0.35 x 10⁶ m³ of lava erupted daily; e.g., Sutton et al., 2003) of this eruption provide a rare opportunity to look beyond the shallow-level crustal processes associated with the short eruptions (days to weeks) that typify many frequently active basaltic volcanoes (e.g., Mauna Loa, Etna, Piton de la Fournaise, Karthala, and Grimsvötn) and into the mantle to reveal melting processes and source heterogeneities (Garcia et al., 2000; Greene et al., 2013).

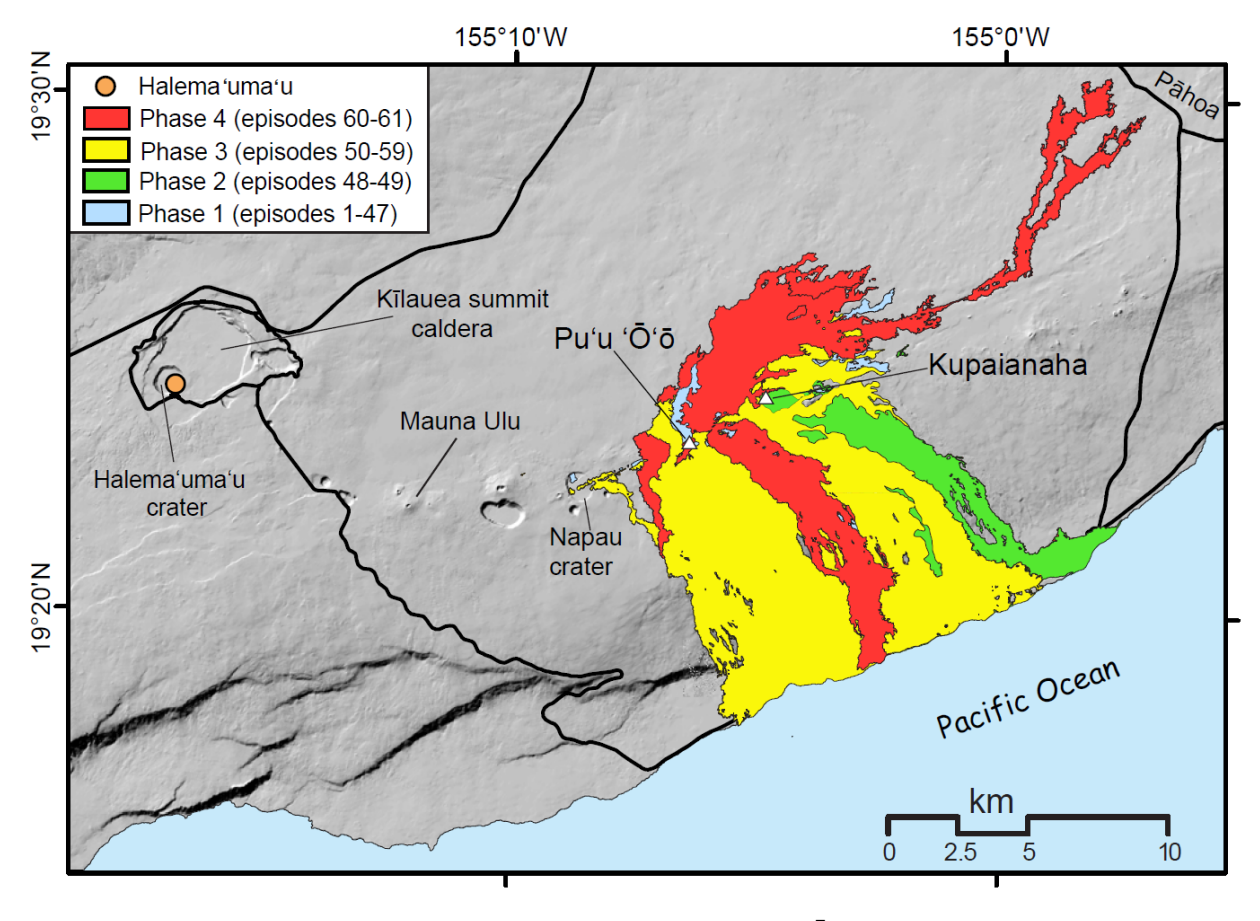


[Figure 1. Map of Kīlauea showing Pu'u 'Ō'ō flow field]

This petrological and geochemical study was initiated in 1983 at the request of the U.S. Geological Survey (USGS) Hawaiian Volcano Observatory (HVO) to rapidly monitor the short term geochemical variations of lava from the Pu'u 'Ō'ō eruption. Many of Kīlauea's previous 20th century rift eruptions lasted only days to a few weeks and producing evolved compositions (<7 wt.% MgO) reflecting magma storage in the rift zone for many years (e.g., Wright and Fiske,1971; Moore et al., 1980; Walker et al., 2019). An eruption on the upper east rift zone at Mauna Ulu from 1969 to 1974 produced more MgO-rich lavas that indicated a conduit had been established between the mantle and the summit reservoir to the vent in the rift zone (e.g., Wright and Tilling, 1980). For our study of Pu'u 'Ō'ō, over a thousand rock samples were collected (mostly in a molten state) to evaluate petrologic and geochemical variations during the eruption. This frequent, real-time sampling occurred on a hourly to weekly basis depending on the extent of observed geochemical variation). Initially, multiple samples were collected in a single day when several fissures were active or when our previous work documented rapid geochemical changes; e.g., Wolfe et al., 1988; Garcia and Wolfe, 1988; Garcia et al., 1989,

1992, 1996). This dynamic sampling scheme allowed the changes in crustal and mantle process during a single, long-lasting magmatic event to be assessed (e.g., Garcia et al., 2000; Pietruszka et al., 2006; Greene et al., 2013; Marske et al., 2008; Walker et al., 2019).

During the Pu'u 'Ō'ō eruption , magma was transported from the mantle to the surface through open channels without significant pooling and homogenization, preserving short-term isotopic and geochemical variations (Pietruszka et al., 2006; Fig. 2). The small size of Kīlauea's summit reservoir compared to the volume of magma produced during the Pu'u 'Ō'ō eruption (≤0.2 vs. ~4.4 km³; Pietruszka et al., 2015; Orr et al., 2015) minimized the buffering effects of mixing with magma stored in the summit reservoir. Thus, the erupted lava closely reflects its parental composition after olivine fractionation (Garcia et al., 2000). The Pu'u 'Ō'ō eruption provides a rare opportunity to sample mantle-derived melts almost continuously over several decades. This time-series analysis of Pu'u 'Ō'ō lavas allowed us to distinguish the dynamic and changing roles of mantle and crustal processes in great detail.

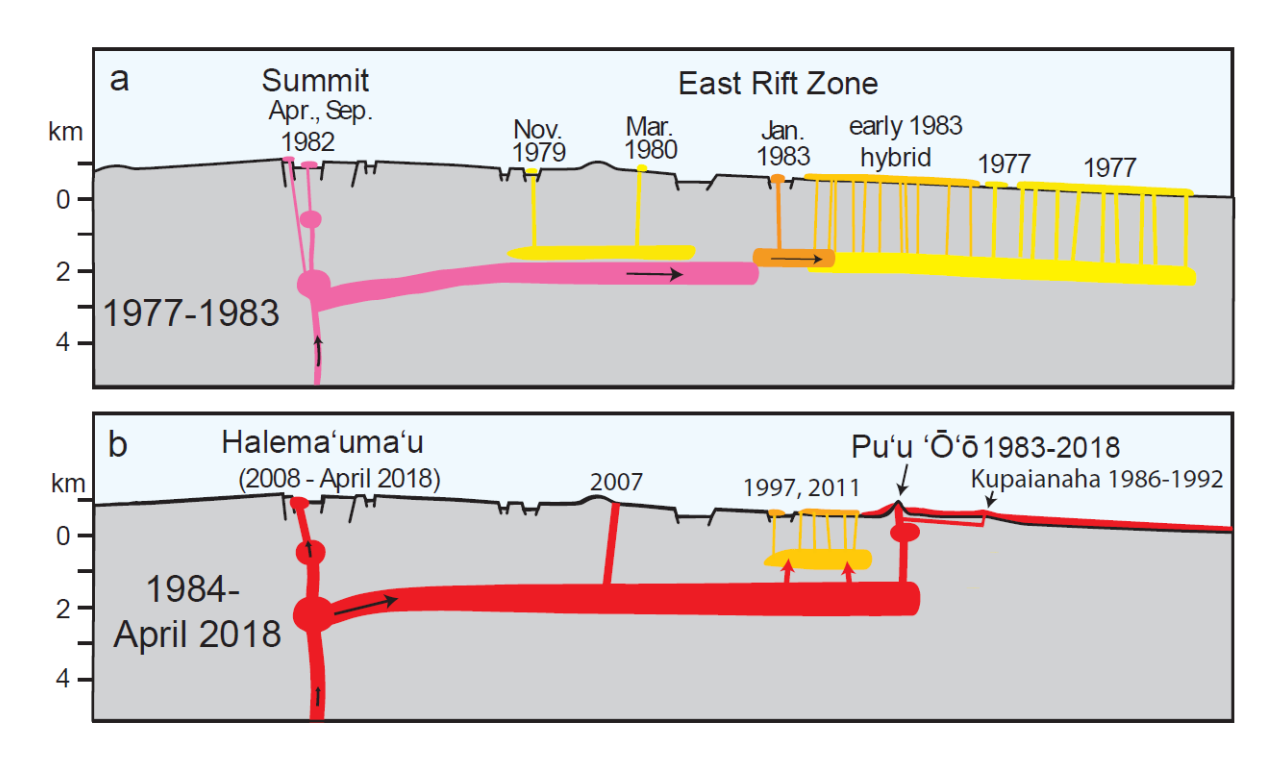


[Figure 2. Cross section of Kīlauea's magmatic system from 1977-2018]

Here we present a synthesis of our volcanological, petrological and geochemical studies of lava and tephra from this remarkable eruption. In addition, new major- and trace-element abundances, and Sr isotope analyses are presented for Pu'u 'Ō'ō lavas erupted from 04 February 2010 to 01 May 2018 (the date of the last sample erupted from the Pu'u 'Ō'ō vent).

These results are evaluated to highlight the major crustal and mantle processes involved in controlling the compositional variations during this long-lived eruption. Also, one of our goals is to make the geoscience community aware of our extensive sample suite (Table S1), and to invite those with a compelling and innovative project to request samples.

113114115

116

117

118

119

120

121

122

123

124

125

126

127128

129

130

131

132

133

134

135

136

137

138

139

140

141

142

143

110

111

112

2. Geologic Background: Kīlauea Volcano and the Pu'u 'Ō'ō Eruption (1983-2018)

Kīlauea volcano is currently in its vigorous, mid-shield building stage (DePaolo and Stolper, 1996; Garcia et al., 2017). It has repayed ~90% of its subaerial surface with tholeiitic lava in <1100 years (Holcomb, 1987). The average historical lava eruption rate of Kīlauea (~0.10 km³/yr; (see Poland et al., 2014 for a summary of magma supply estimates) is one of the highest of any volcano on Earth. Shield-stage magma is thought to originate by partial melting at depths >70 km within the Hawaiian mantle plume (Watson and McKenzie, 1991; Tilling and Dvorak, 1993; Wright and Klein, 2006) and transported through the upper mantle via chemicallyisolated channels (Pietruszka et al., 2006). These channels merge into a conduit that currently supplies a shallow (2-6 km) summit reservoir complex that consists of two magmatic bodies (e.g., Poland et al. 2014; Pietruszka et al., 2015). Estimates for the volume of these bodies based on geophysical methods vary widely: ~0.1–7.2 km³ for the shallower (1-2 km depth) Halema'uma'u magma body and ~13-27 km³ for the deeper south caldera reservoir (Poland et al., 2014; Anderson et al., 2015; 2019). However, variations in Pb isotope ratios for historical summit lavas indicate a much smaller volume for the two bodies (0.06-0.2 km³ from 1971 to 1982; Pietruszka et al., 2015). The discrepancy between geochemical vs. geophysical can be reconciled if the geophysics-based estimates include an olivine-rich crystal-mush zone and hot, ductile rocks that surround the summit reservoir, whereas the estimates based on the Pb isotope ratios represent only the molten core of the reservoir where magma is mixed (Pietruszka et al., 2015). The residence time of magma within the summit reservoir complex is relatively short (~0.5-1 year; Pietruszka et al., 2015). Kīlauea's historical (post-1820) eruptions occurred mostly at or near the summit prior to 1955 (Garcia, 2015). Subsequently, rift zone eruptions became more common, especially along the east rift zone, including the 1969-1974 Mauna Ulu eruption, which was the most voluminous historical eruption prior to Pu'u 'Ō'ō (Macdonald et al., 1983).

The Pu'u 'Ō'ō eruption was Kīlauea's most important historical eruption. Details of its chronology are given in the excellent reports by Wolfe et al. (1988), Heliker and Mattox (2003) and Orr et al. (2015). A brief summary is given here highlighting the main features of the eruption. Eruption rates were high and variable from 1983-2002 (e.g., Sutton et al., 2003).

Magma supply rates to the east rift zone are thought to have nearly doubled during 2003–2007 (~0.11 to at least 0.19 km³ yr⁻¹; Poland et al., 2012), although a more recent estimate suggests a range of 60-150% increase (Anderson and Poland, 2016). After 2007, eruption rates were lower, perhaps similar to the pre-2000 rates (Anderson and Poland, 2016). Not all of the magma supplied to of Kīlauea is erupted; it is estimated that only ~1/3 was erupted during the 20th century (e.g., Dzursin et al., 1984). Typically, much of Kīlauea's mantle-derived magma is stored in the summit reservoir or injected into the rift zones (Poland et al., 2014). Thus, eruption rates are not equal to magma supply rates and both are highly variable. However, during the Pu'u 'Ō'ō eruption at least half (perhaps nearly all) of the magma that entered Kīlauea was erupted from 2000-2012, the period examined by Anderson and Poland (2016). Variations in mantle-derived magma supply rate may be due to pulses of magma generation (e.g., Garcia et al., 1996) or withdrawal of magma from Kīlauea's summit reservoir system (by eruption or intrusion into the rift zones) that unloads the magma plumbing system and triggers magma ascent from the mantle (Dzurisin et al., 1984). Most importantly for interpreting the geochemical variations during the Pu'u 'Ō'ō eruption, new magma was essentially continuously supplied from the mantle (Greene et al., 2013; Anderson and Poland, 2016). However, estimates of magma supply rate and interpretations of the geochemical evolution of erupted lavas are complicated by numerous factors including uncertainties in the volume of magma stored within the deep portions of Kīlauea's rift zones (this volume is difficult to detect) and the compressibility of magma (Anderson and Poland, 2016). Thus, our efforts in this paper to correlate geochemical variations with magma supply rates are qualitative.

The Pu'u 'Ō'ō eruption was triggered on 02 January 1983 with the intrusion of a dike from Kīlauea's upper east rift zone (Fig. 2). The intrusion was followed 24 hours later by eruptive activity along a discontinuous, 7 km long fissure (episode 1; Wolfe et al., 1987). Effusion localized six months later at a central vent, Pu'u 'Ō'ō (Figs. 1 and 2). The USGS subdivided the entire eruption into 61 'episodes', although some episodes were further subdivided with letters (episode 61 had seven parts). Each episode either follows a break in eruptive activity or a shift in vent location (e.g., Wolfe et al., 1988; Heliker and Mattox, 2003). Some of these episodes were coeval (e.g., 48 and 49) or reflect a minor change in the vent location (e.g., flanks vs. interior of the Pu'u 'Ō'ō cone). Here, we divide the eruption into four main phases based on eruptive style and vent location: Phase 1 (episodes 1-47), Phase 2 (episode 48-49), Phase 3 (episodes 50-59), and Phase 4 (episodes 60-61).

The details of Phases 1 and 2 are well documented in published papers; thus, they are only briefly described here. Phase 1 (January 1983 to June 1986, days 1-1,270) involved brief

(mostly less than 24 hours), remarkably episodic eruptions that occurred mainly at the Pu'u 'Ō'ō vent with repose periods averaging 24 days (Wolfe et al., 1987, 1988; Heliker and Mattox, 2003). Phase 2 (July 1986 to February 1992, days 1,299-3,320) had nearly continuous effusion at the Kupaianaha vent (Fig. 2), about 3 km downrift (east) from Pu'u 'Ō'ō cone (episode 48; Heliker et al. 1998; Heliker and Mattox, 2003). This new vent was fed by a shallow (<100 m deep) conduit from Pu'u 'Ō'ō that allowed partially degassed magma to be erupted (Garcia et al., 1996). A brief (~18 day) lava outbreak occurred between the Pu'u 'Ō'ō cone and Kupaianaha crater in Nov. 1991 (episode 49) while the Kupaianaha vent was active.

178

179

180

181

182

183

184

185

186

187

188

189

190

191

192

193

194

195

196

197

198

199

200

201

202

203

204

205

206

207

208

209

210

211

Phase 3 (Feb. 1992 to March 2011, days 3,333-10,289) also had nearly continuous effusion mostly from vents within or on the flanks of the Pu'u 'Ō'ō cone (Orr et al., 2015). However, three, uprift (to the west and closer to the summit; Fig. 1) eruptions happened during Phase 3 (episodes 54, 56 and 59). Episode 54 occurred on 29 January 1997. It was accompanied by a 150 m collapse of Pu'u 'Ō'ō crater floor. This was followed immediately by formation of a 2.5 km long discontinuous fissure system 2-4 km uprift of Pu'u 'Ō'ō that was active for less than a day (Harris et al., 1997; Heliker and Mattox, 2003). It produced evolved magma (<7 wt.% MgO) that had been stored in pockets along the rift (Garcia et al., 2000; Thornber et al. 2003). A six-week hiatus in effusive activity followed episode 54. Glow was observed at the Pu'u 'Ō'ō vent on 24 February 1997, which started episode 55. It was shortlived with Episode 56 occurring 17 June 2007 two days after an ~80 m collapse of the Pu'u 'Ō'ō crater floor and a dike intrusion from the upper east rift zone. The vent for this brief (few hours), small (~1500 m³) eruption was ~6 km uprift from Pu'u 'Ō'ō (Montgomery-Brown et al., 2010). It was followed by a 12-day pause in the eruption. Lava production resumed for three weeks in and around Pu'u 'Ō'ō cone (episode 57) until 21 July 2007, when a fissure opened on the east flank of Pu'u 'Ō'ō and propagated eastward 2 km towards the Kupaianaha vent (Figure 1; Table 1). This marked the beginning of episode 58 (Orr et al., 2015), which continued through March 2011, mostly as tube-fed flows from a vent ~2 km east of Pu'u 'Ō'ō. Lava output waned in 2010, but in early 2011, seismicity and lava lake levels at the summit and Pu'u 'Ō'ō crater increased. The third uprift eruption (episode 59) occurred on 05 March 2011 and lasted four days. The 2 km long, episode 59 fissure system had two segments (east and west); they formed only 10's m south of the episode 54 fissures (Orr et al., 2015; Thornber et al., 2015; Walker et al., 2019). A few days after episode 59 ended, the eruptive activity resumed (episode 60) at the Pu'u 'Ō'ō vent.

Phase 4 (March 2011 to May 2018, days 10,298-12,903) had virtually continuous effusion after the 12-day hiatus following episode 59. The Pu'u 'Ō'ō eruption waxed and waned for the

next several years until new fissures formed on the east flank of Pu'u 'Ō'ō on 27 June 2014. These fissures produced a rapidly advancing flow that traveled 20 km east into the community of Pāhoa between July and late October 2014 (Fig. 1). This flow nearly cut off the only highway for about 10,000 residents before it stagnated on the gentle slopes just uphill from the Pāhoa community in mid-December 2014. Eruptive activity refocused around Pu'u 'Ō'ō until the end of the eruption on 01 May 2018, when the floor of the crater collapsed and magma propagated 20 km downrift and erupted along the lower east rift zone (Neal et al., 2018).

Kīlauea's other notable eruptive activity during the Pu'u 'Ō'ō eruption was the Halema'uma'u eruption at its summit (Figs. 1 and 2) that started in March 2008 during Phase 3 (e.g., Patrick et al., 2015). The summit lava lake activity continued during Phase 4 and ended with the collapse of the summit lava lake on 02 May 2018, a day after the Pu'u 'Ō'ō eruption ended (Neal et al., 2018). The lake level during this decade of activity fluctuated >100 m and overflowed twice onto the main floor of Halema'uma'u. The lake had numerous small explosive events related to collapse of its crater walls (Patrick et al., 2013).

3. Sample Description

Samples utilized in this study were obtained from both the USGS collection, especially from Phase one (1983-1986), and by our team assisted by numerous volunteers. An inventory of all the samples collected (not all were chemically analyzed) and used for this study is given in the data supplement (Table S1). Most samples were collected molten with a rock hammer (for surface flows) or a 15 cm long steel pipe at the end of a 5-50 m long steel chain or cable (for sampling the Kupaianaha lava lake and lava tubes). Samples were usually water quenched to minimize post-eruptive crystallization. This resulted in a glassy, strongly vesicular (>50 vol.%) and friable sample. However, water quenching was not possible for some samples, especially from episode 54 when samples were collected after they had air cooled. In these cases, samples were collected near the vent or from the glassy outer surface of lava flows for which a date of eruption was known within a day or two. Some samples of episodes 40 and 46 (Phase 1) were collected as tephra; they are labeled with a T after the sample number in Table S1. Samples from the USGS collection have unique numbers (e.g., KE30-361) that indicate their eruptive episode (as defined by the USGS) and order of collection. The order of collection was sometimes long after the sample was erupted. The names for our samples are given by the collection date (e.g., day-month-year), which is generally within less than a day of its eruption (when lava was flowing in open channels on the surface or in lava tubes; Garcia et al. 2000), or up to a week or more when it was oozing slowly within advancing pāhoehoe flows on the

coastal plain. When multiple samples were taken on a single day, the time of collection was added to the inventory (Table S1).

3.1. Petrography

Most Pu'u 'Ō'ō samples are petrographically simple: aphryic to weakly phyric with <1 to 3 vol.% of small, euhedral olivine phenocrysts (0.5-1 mm) and microphenocrysts (0.1-0.5 mm; Fig. 3A). Some olivine crystals contain tiny (<0.1 mm) chromite inclusions (Fig. 3A and 3B). These crystals occur within a glassy or cryptocrystalline matrix that may also contain microphenocrysts of clinopyroxene and plagioclase. Lava from episodes 1-10, 54 and 59 contain resorbed crystals (Garcia et al., 1989; 1992; 2000; Walker et al., 2019). A few samples from other episodes collected on the coastal plain >10 km from the vent contain abundant olivine (5-10 vol.%; Fig. 2B) due to concentration during surface flow. Some samples with more evolved compositions (<7 wt.% MgO) have sparse (<2 vol.%) phenocrysts of clinopyroxene and plagioclase microphenocrysts (Fig. 23C). Gabbroic crystal clots (clusters of plagioclase, clinopyroxene and spinel commonly with interstitial glass; Fig. 3D) are found in some of the 2011-2018 lavas. These clots affected the lava composition as discussed below. More detailed petrographic descriptions of some of the samples used in this study can be found in Garcia and Wolfe (1988), Garcia et al. (1989; 1992; 1996; 2000), and Marske et al. (2008). For other petrographic descriptions of Pu'u 'Ō'ō lava, see Thornber et al. (2003, 2015).

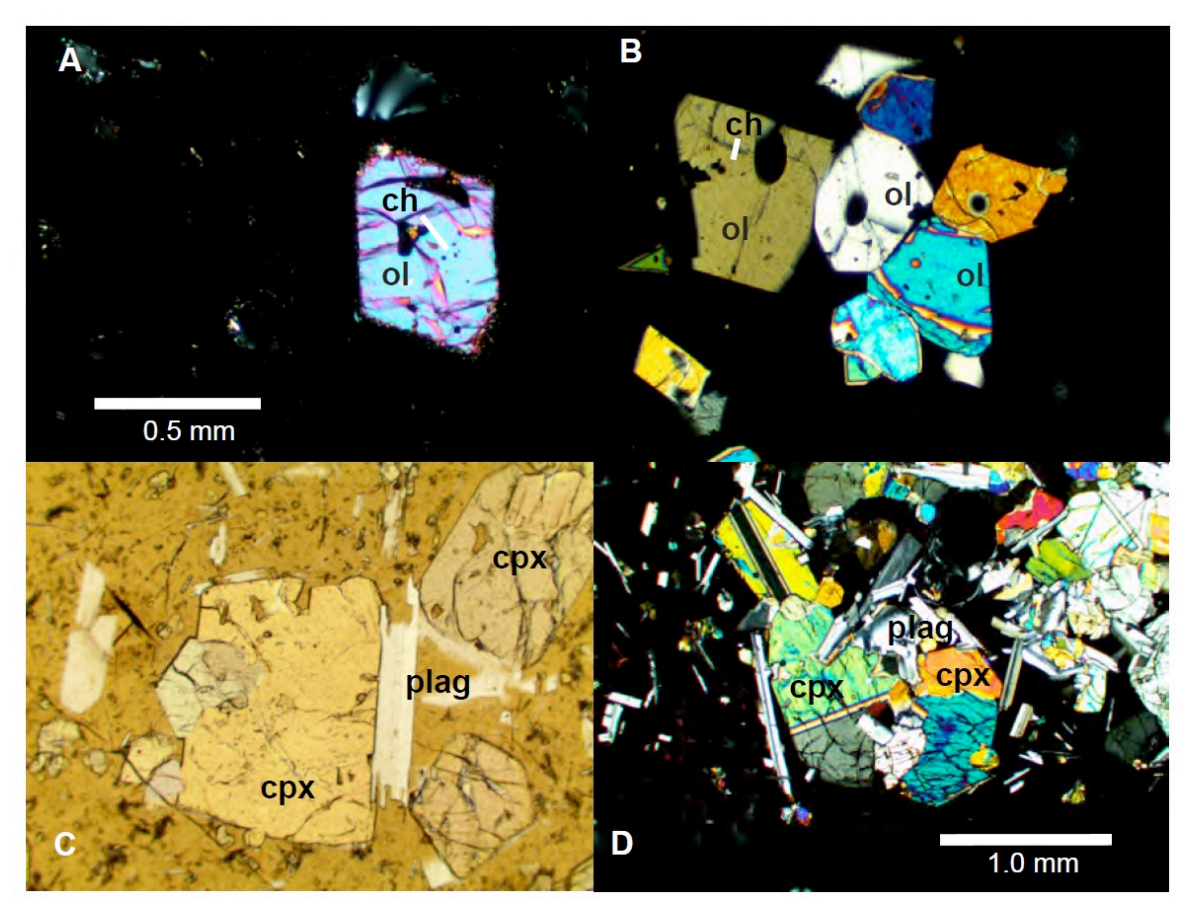


[Figure 3. Panel of 4 photomicrographs of Pu'u 'Ō'ō lava]

One notable feature of Pu'u 'Ō'ō lavas is the presence of olivine phenocrysts and microphenocrysts that are generally in equilibrium with the bulk rock composition, except in samples with bulk rock Mg# >61 (Garcia et al., 1996; 2000; Marske et al., 2008). These higher Mg# samples contain more olivine (Fig. 3B); thus, they probably accumulated olivine. Equilibrium between olivine crystals and their host whole-rock composition is also observed for many, weakly olivine-phyric, historical Kīlauea summit lavas (Garcia et al., 2003).

4. Analytical Methods

We analyzed 656 Pu'u 'Ō'ō volcanic rock samples (264 are new analyses; all analyzes after 22 Jan 2010) for major and the trace elements (Sr, Y, Zr, Nb, Rb, Ba, Zn, Ni, Cr, V; Supplemental Table S2) by X-Ray Fluorescence Spectrometry (XRF). The XRF analyses were performed at the University of Massachusetts at Amherst (see Rhodes, 1996; Rhodes and Vollinger, 2004 for procedural methods). The samples were coarsely crushed (1-8 mm) with a tungsten-carbide coated hydraulic press, ultrasonically cleaned in Millipore water, then dried for

24 hours at 40°C. Samples were hand-picked to remove fragments with signs of alteration or foreign material to ensure only the freshest parts of each sample were analyzed.

The accuracy and analytical precision for these analyses is based on replicate measurements of the BHVO-1 Hawaiian basaltic reference material throughout the 3.5 decades of the eruption (see supplemental Table S3) involving numerous re-calibrations, three X-ray spectrometers, and many different flux batches for the major elements. These data are calibrated relative to BHVO-1 in preference to BHVO-2 because at the start of this project BHVO-2 did not exist.

In addition, we present 41 new ICPMS trace element analyses representing eruption dates from 29 Jan. 2006 through 01 May 2018 (Table S2). The new analyses were conducted at the Research School of Earth Sciences (RSES), Australian National University (ANU), and were obtained by solution-aspiration quadrupole or magnetic-sector inductively-coupled plasma mass spectrometry (ICPMS). For these analyses, separate splits of the Pu'u 'O'o lava samples were washed in an ultrasonic bath of deionized water for 10-20 min, hand-picked (30-100 g) to remove any altered rock chips, and powdered in an agate mill. Approximately 50 mg splits of the powders were dissolved in distilled HF-HNO3 and brought to a final volume of 100 ml with 2% HNO3 for analysis. The final solutions contained ~50 ppb Be and 5 ppb each of In, Re, and Bi as internal standards that were used to correct for instrument drift. The Kīlauea reference basalt BHVO-2 was used for calibration of element sensitivities, and the USGS reference basalts W-2, DNC-1, and BIR-1, additional splits of BHVO-2, and replicate solutions of the in-house reference basalts Kil1919 (a re-collection of the same flow from which BHVO-2 was prepared; Rhodes and Vollinger, 2004) and KIL93 (collected from a Pu'u 'O'o flow on 10 May 1993; Eggins et al 1997) were analyzed with the unknowns for quality control (Table S4).

A compilation was made (Table S2) of our Pu'u 'Ō'ō ICPMS trace element data including those published previously by Garcia et al. (1996; 60 analyses obtained at Washington State University) and Marske et al. (2008; 28 analyses obtained at ANU). The data were corrected to a consistent set of calibration values for BHVO-1 and BHVO-2 (Table S4). Greene et al. (2013) provide new ICPMS trace element data for 13 samples erupted during 1983-1984 and 2007-2010. However, these data could not be corrected to be consistent in detail with the WSU and ANU data with the information provided and are not included in this compilation.

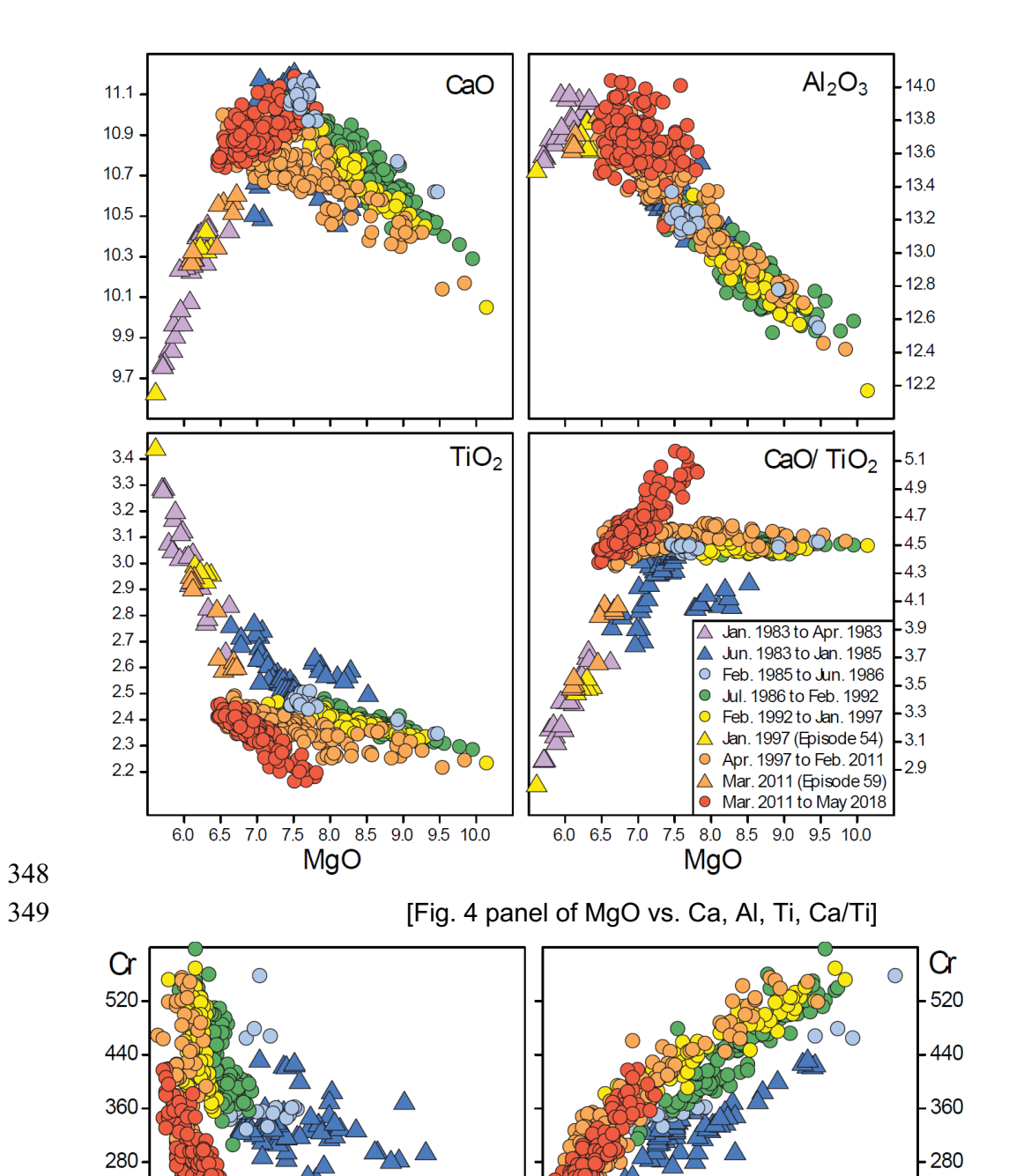
New strontium isotopic compositions for 26 samples obtained from 2010-2018 were measured with a TritonPlus thermal ionization mass spectrometer at RSES. The chemistry was done in a class 1000 clean lab using Teflon distilled reagents. None of the Pu'u 'O'o samples or reference materials were leached before analysis. Powder aliquots (~10 mg) were weighed and

dissolved in HF-HNO3. Strontium was extracted from the matrix using 300 μ l shrink-Teflon columns filled with 200 μ l Eichrom Sr-spec resin and 100 μ l of prefilter resin using a slightly modified procedure after Deniel and Pin (2001). Procedural blanks were 10-20 picrograms and therefore, are negligible. Approximately 200 ng of Sr from each sample was loaded on a single zone-refined, outgassed Re filament using a TaF5 activator. Samples were run in static mode typically at 4-9 volts of ⁸⁸Sr using 10¹¹ ohm resistors and monitoring ⁸⁵Rb for potential interferences at ⁸⁷Sr. Each analysis comprised 200-300 cycles with 8 sec integration times, and was normalized to ⁸⁸Sr/⁸⁶Sr = 8.375209 to correct for mass fractionation during the run. The average measured ⁸⁷Sr/⁸⁶Sr in SRM987 during the time that these new Pu'u 'Ō'ō analyses were obtained was 0.710260 \pm 0.000020 (2SD, n = 27). Previously published data (Marske et al., 2008; Greene et al., 2013; Pietruszka et al., 2018) were compiled and all of the Sr isotopic data were corrected to an ⁸⁷Sr/⁸⁶Sr ratio of 0.710250 for SRM987 (Table S5). Results are also provided for reference material Kil93 and compared to values reported by Nobre-Silva et al. (2013).

5. Results and Discussion

5.1. Whole Rock XRF Major and Trace Element Chemistry: Overview

Pu'u 'Ō'ō basalts are compositionally heterogeneous (e.g., 5.6-10.1 wt.% MgO and 0.35 to 0.72 wt.% K₂O; Table S2). Their range in composition is well illustrated in MgO variation plots because Mg-rich olivine is the primary mineral in these lavas. Plots of CaO, Al₂O₃, and CaO/TiO₂ vs. MgO show nearly linear trends at higher MgO (>7.5 wt.%; Fig. 4). At lower MgO values, there are inflections in these trends that reflect the fractionation of clinopyroxene starting at ~7.5 wt.% MgO and plagioclase at ~6.5 wt.% MgO (Fig. 4). The role of these minerals in the crystallization sequence is confirmed by their presence as microphenocrysts and rarely as phenocrysts in the lower MgO basalts (Garcia and Wolfe, 1988; Garcia et al., 1989, 1992). In addition, the plots of CaO and TiO₂ vs. MgO illustrate the temporal variations in parental magma composition (e.g., differences in CaO and TiO₂ at a given MgO value >7.5 wt.%). Systematic temporal variations can also be seen in plots Cr vs. Nb and Ni (Fig. 5). Some of the geochemical variations (MgO) occurred over short timescales (i.e., hours to days) during Phase 1, whereas ratios of incompatible trace elements varied over months to decades during each of the phases (Garcia et al., 1989; 1992; 1996; 2000; Marske et al., 2008; Greene et al., 2013).



Nb

[Fig. 5 side by side plot of Nb and Ni vs. Cr]

100 120 140 160 180 200

Ni

- 200

- 120

In the next section, the major element compositions of Pu'u 'Ō'ō lavas are discussed with an emphasis on crustal processes. Initially, the compositional variation involved mixing of new, mantle-derived, olivine-saturated magma (>7 wt.% MgO) with fractionated magma that had experienced multi-phase crystal fractionation and was stored in the rift zone (<7 wt.% MgO). The Phase 1 and 2 results and interpretations are drawn largely from our previous papers. The Phase 3 and 4 sections include new geochemical results for the 2010-2018 portion of the eruption (days 9924-12,901).

5.2. Temporal Geochemical Variations in Crustal Processes

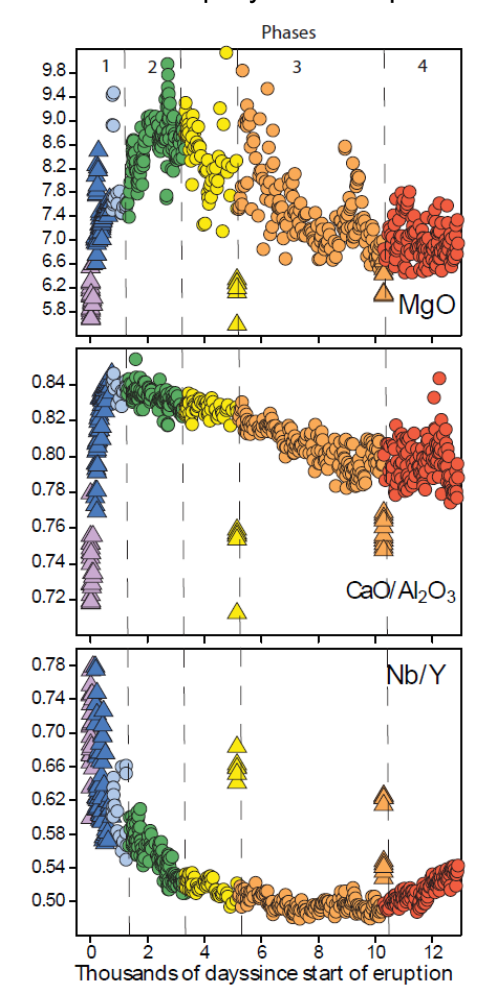
The temporal variations in whole-rock XRF data are discussed below in the context of the four main volcanological phases of the Pu'u 'Ō'ō eruption, as described above. These data are interpreted mostly in the context of crustal processes such as crystal fractionation and mixing. Oxygen isotope data are also discussed to address the role of crustal assimilation based on our previously published oxygen isotope data days 1-5121 (January 1983 to January 1997; Garcia et al., 1998). This is followed by a discussion on parental magma composition variations during the eruption.

5.2.1. Phase 1: 1983-1986 (days 1-1271)

Petrographic and compositional evidence in the earliest Pu'u 'Ō'ō lava (<300 days) indicates that the two most important magmatic processes were pre-eruptive crystal fractionation followed by syn-eruptive magma mixing (Garcia et al., 1992). The pre-eruptive fractionation produced differentiated magmas (<7 wt.% MgO and phenocrysts of clinopyroxene and less commonly plagioclase) within the rift zone (Garcia and Wolfe, 1988). These magmas were mixed during the start of the eruption as a new dike was intruded from the upper east rift zone as demonstrated by the presence of resorbed olivine and plagioclase, and linear compositional trends that are oblique to the olivine-controlled trends, especially in some 1983 lavas (Garcia et al., 1989; 1992). Magma in the intruding dike was hotter and more MgO-rich (>7 wt.%; Wolfe et al., 1988). The new dike forced mixing of two cooler, differentiated magmas that had been stored in the rift zone for decades (Garcia et al., 1989). The resulting hybrid magmas resided in a shallow reservoir under the Pu'u 'Ō'ō vent that was replenished between eruptive episodes with new, more MgO-rich magma from the summit (Hoffman et al., 1990; Garcia et al., 1992). During episodes 4-47 (days 161-1270), the upper part of this reservoir was tapped to produce weakly olivine-phyric lava with rare or no clinopyroxene microphenocysts (<0.5 mm across). This is a common lithology on Hawaiian shield volcanoes and has been

called "reservoir type magma" (Rhodes, 1988). It is a cotectic composition (~7.5 wt.% MgO) reflecting the thermal balance between cooling and the heat from crystallization for olivine and clinopyroxene. More MgO-rich magma (9.5 wt.%) was erupted during two, high-volume early episodes (30 and 31) with sharp transitions over ~1-hr. periods from 7.6 to 9.4 wt.% MgO (Mittelstaedt and Garcia, 2007). This implies a ~35°C change in temperature based on the MgO glass thermometer of Helz and Thornber (1987).

Rapid (hours to days) variations in MgO are recorded in the early Pu'u 'Ō'ō lava (Jan. 1983 to May 1984, days 1-500; Fig. 6). These lavas were produced during usually brief (typically 1-2 day) events with geyser-like lava fountains (up to 400+ m high) that partially evacuated the dikelike, shallow magma reservoir system under the Pu'u 'Ō'ō vent (Wolfe et al. 1988; Hoffmann et al., 1990; Shamberger and Garcia, 2007). All but one of the earliest lavas (days 1-96) have lower MgO (~5.7-6.3 wt.%) as well as low CaO/TiO₂ (3.0-3.7) and elevated concentrations of incompatible elements such as TiO₂ (Fig. 3). The lowest MgO lavas are compositionally identical to those from the nearby 1977 Kīlauea eruption (Garcia et al., 1989). Subsequent lavas transitioned rapidly to more primitive compositions with higher MgO and CaO/TiO₂, and lower



387

388

389

390

391

392

393

394

395

396

397

398

399

400

401

concentrations of incompatible elements with 90% of the variation within the first 400 days of the eruption (Shamberger and Garcia, 2007). During this time, the ²⁰⁶Pb/²⁰⁴Pb ratios of Pu'u 'Ō'ō lavas display a rapid temporal decrease as the stored magma was flushed from the ERZ (Greene et al., 2013). There were also changes in lava composition over short timescales (hours to days) that cannot be due to processes such as mantle melting, source variations, fractional or crystallization in a static magma chamber. Instead, a rapid flushing and mixing with the resident magma in the Pu'u 'Ō'ō reservoir by new, more MgO-rich magma is required (Garcia et al., 1989; 1992). Lavas erupted after day ~500 show no petrographic or geochemical evidence for magma mixing (Shamberger and Garcia, 2007) until the 1997 uprift eruption (episode 49, day 5141).

[Fig. 6 Time vs. MgO, Ca/Al, and Nb/Y]

Crustal assimilation was an important process during Phase 1 based on oxygen isotope data for olivine and glass separates from these rocks. Glass oxygen isotope values were low $(\delta^{18}O < 5.0\%; Table S2)$ and olivine-glass differences were all \leq -0.15% (except one at -0.35%) indicating disequilibrium and recent assimilation (Garcia et al., 1998). Assimilation had little or no effect on the whole rock chemistry based on the lack of correlation between whole-rock chemistry with oxygen isotope ratios (Garcia et al., 1998). Thus, the assailant was probably Kīlauea lava.

5.2.2. Phase 2: Shift to the Kupaianaha vent (1986 to 1992, days 1300 to 3320)

The locus of extrusion shifted 3 km downrift (east) to the Kupaianaha vent (Figs. 1 and 2) on day ~1300. Lavas erupted at this vent show a wide range in MgO (Fig. 5) that is related to three changes in volcanic behavior: (1) Eruption style went from episodic to continuous effusion following the shift in vent location in mid-1986; (2) the pulsating supply of magma from Kīlauea's summit reservoir; and (3) brief hiatuses (1-4 days) in effusion (Garcia et al., 1996). The shift to nearly continuous effusion in mid-1986 resulted in a rapid, ~1 wt.% increase in MgO as magma avoided storage (typically for one month) in the shallow and open Pu'u 'Ō'ō reservoir between eruptions, allowing compositionally more primitive but weakly olivine-phyric (<1 vol.%) lava to be erupted. During periods of continuous effusion, changes in summit tilt recorded the fluctuating flux of magma from the mantle. These fluctuations were followed ~19 days later by small (0.5 wt.%) increases or decreases in MgO content that correlate with summit inflation or deflation. The change in MgO reflected the extent of cooling (olivine fractionation) of the magma during transport within the rift zone (Garcia et al., 1996). The 1-4 day hiatuses led to fractionation of olivine in the shallow magma reservoir resulting in the lava erupted after the hiatus having lower MgO followed by higher MgO (up to 2 wt.% variation) in later lava from the accumulation of olivine (Garcia et al., 1996).

Crustal assimilation was less during Phase 2. Matrix δ^{18} O values were 5.03-5.25‰ (for six samples) vs. <5.0‰ for Phase 1 (Table S2). During the first 200 days of Phase 2, matrix values were higher (5.2‰) and olivine-matrix values were -0.7‰ (typical equilibrium value) for two samples (Garcia et al., 1998). However, matrix glass δ^{18} O decreased during Phase 2 (5.03-5.11‰) and olivine-matrix decreased to -0.3‰ indicating that coeval olivine did not grow in these melts (Garcia et al., 1998).

5.2.3. Phase 3: Back to Pu'u 'Ō'ō vent (Feb. 1992 to March 2011, days 3333-10,289)

Lavas erupted at the start of Phase 3 are compositionally continuous with those at the end of Phase 2, with relatively high MgO (8.0-9.2 wt.%) and Ni (140-170 ppm), and similar concentrations of incompatible elements (Table S2; Figs. 5 and 6). This is because the Kupaianaha vent was fed by a shallow dike from the Pu'u 'Ō'ō reservoir (Garcia et al., 1996). As this eruptive phase progressed, MgO and Ni concentrations declined slowly until reaching a relatively constant composition (~7 wt.% and 80 ppm, respectively) by day ~8000 in 2005 despite the major increase in magma supply rate from days 7300 to 8900 (2003 to 2007; Poland et al., 2012). We expected to see the MgO content increase with the increase in magma supply based on the trend during Phase 2. Instead, MgO remained relatively low during this surge in magma supply (Fig. 4). There were occasional spikes to higher MgO compositions (e.g., days ~5400-5500 and ~6200) in lavas collected on the coastal plain 8-10 km from the vent. These spikes reflect an increase in olivine abundance during flow. There was no change in the oxygen isotope values during this phase (Garcia et al., 1998).

Three, short-lived (<1 to 4 days) eruptions occurred uprift (west) of the Pu'u 'Ō'ō vent in 1997 (day 5141), 2007 (day 8932) and 2011 (days 10,290-10,293; Fig. 2). The 1997 (episode 54) and 2011 (episode 59) eruptions occurred 2-4 km west of the Pu'u 'Ō'ō vent. Their fissures are only 10's of meters apart whereas the 2007 (episode 56) eruption was 6 km west of Pu'u 'Ō'ō. Episodes 54 and 56 occurred immediately after a major collapse (10's of meters) of the Pu'u 'Ō'ō crater floor. Episode 56 was triggered by a dike intrusion from the middle east rift zone (Orr et al., 2015). The lavas from episodes 54 and 59 are petrographically and compositionally distinct from coeval Pu'u 'Ō'ō lava. They contain resorbed and reversely zoned minerals (Garcia et al., 2000; Walker et al., 2019), and lower MgO (5.6-6.4 vs. 7.5-10.1 wt.%) and CaO/Al₂O₃ (0.77-0.70 vs. 0.79-0.82; Figs. 4 and 5); these features are seen in the early Phase 1 lava (Garcia et al., 1989; 1992). These features are thought to result from mixing Pu'u 'Ō'ō magma with stored, differentiated rift zone magma (Garcia et al., 2000; Thornber et al., 2003; Walker et al. 2019). In contrast, episode 56 lavas have higher MgO than coeval Pu'u 'Ō'ō lava (8.5 vs. 7.2 wt.%) but are otherwise geochemically indistinguishable from contemporaneous Pu'u 'Ō'ō lavas (Fig. 5; Table S2).

Oxygen isotope values are low for the first two years of Phase 3 (~5.0‰ for four samples, days 3440-4131; Table S2). Values for olivine-matrix were also low (~-0.3‰ for the two analyzed samples; Garcia et al., 1998;). A year later in 1995 (day ~4500) matrix values increased slightly to ~5.2‰ and olivine-matrix values were at or nearer equilibrium values (0.5-0.7‰) indicating that the olivine grew in the host melt (Garcia et al., 1998). Two subsequent samples showed the same results (days 4765 and 5121). Although the matrix values for

samples from Phases 2 and 3 are low compared to assumed mantle values (5.03-5.25 vs. 5.5‰), they are typical of the values for Kīlauea summit lavas erupted just before the start of the Pu'u 'Ō'ō eruption (1954-1982; Garcia et al., 2008).

5.2.4. Phase 4: (March 2011 to May 2018, days 10,298-12,903)

The lava during this phase have generally lower and more restricted MgO contents (6.5-8 wt.%) with most values <7.0 Wt% MgO (Table S2). However, the overall compositions are more variable due to the presence of gabbroic clots (Fig. 3). These clots are common (up to ~5 vol.%), and they impart anomalous geochemical trends compared to lava without them (e.g., higher MgO, Al₂O₃, CaO, and CaO/TiO₂ and lower TiO₂; Figs. 4 and 5, Table S2). However, trace element ratios that are insensitive to gabbroic clots (e.g., Nb/Y; Fig. 6) indicate that Phase 4 was a period of increasing concentrations of incompatible elements that reversed the long-term decreasing trend (Fig. 6). This geochemical reversal was probably related to a change in parental magma composition likely related to source composition or conditions of melting.

6. Parental Magma Variations

Historically, Kīlauea has been supplied nearly continuously from the mantle with compositionally variable magma (e.g., Wright, 1971; Pietruszka and Garcia, 1999; Garcia et al., 2003). For example, lava from the 1969-1974 upper east rift eruption at Mauna Ulu showed small but systematic changes in parental magma composition (Hofmann et al., 1984; Pietruszka et al., 2018). Multiple factors led us to anticipate substantial parent magma variations for the Pu'u 'Ō'ō eruption: 1. Its high eruption rate; 2. The nearly continuous effusion over 35 years; and 3. The relatively small size of the late 20th century summit magma storage reservoir compared to the volume of this eruption (<1 km³ vs. >4 km³; Pietruszka et al., 2015; Orr et al., 2015). Thus, any short-term geochemical fluctuations in the mantle source would be effectively transported to the surface (Greene et al., 2013). Accordingly, we expected the parental magma composition to change. However, the observed variations were greater and more complicated than expected.

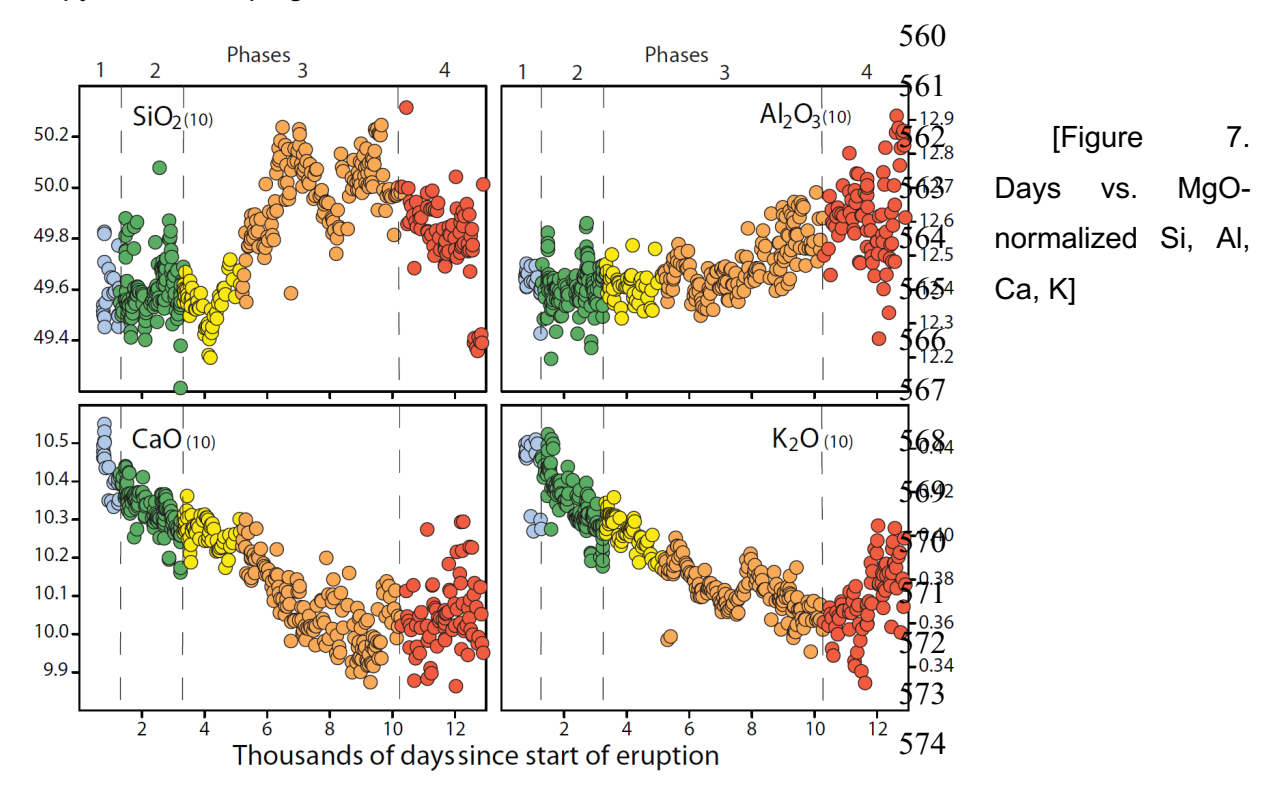
The Pb isotope ratios of Pu'u 'Ō'ō lavas from 1983 to 2012 were used to estimate the transport time magma from the summit reservoir to the ERZ and pinpoint the arrival of a new mantle-derived magma batch to Kīlauea's shallow plumbing system (Pietruszka et al., 2018). The ²⁰⁶Pb/²⁰⁴Pb ratios of Pu'u 'Ō'ō lavas decreased rapidly from 1984 until they reached a minimum from 1988 to 1990 (Greene et al., 2013). Modeling of this temporal decrease in ²⁰⁶Pb/²⁰⁴Pb suggests a magma residence time of ~2 years and a magma volume of ~0.2

km³ (Pietruszka et al., 2018), which likely represents the small amount of magma that was undergoing mixing within both the summit reservoir and the ERZ during this time. Thus, most of the pre-1983 stored magma was likely flushed from the summit reservoir during the first few years of the Pu'u 'Ō'ō eruption by a new, mantle-derived parental magma with a low ²⁰⁶Pb/²⁰⁴Pb ratio. This isotopically distinct melt was delivered after the Sep. 1982 summit eruption (Pietruszka et al., 2015). It may have arrived with the dike intrusion that initiated the Pu'u 'Ō'ō eruption in Jan. 1983. The ²⁰⁶Pb/²⁰⁴Pb ratios of Pu'u 'Ō'ō lavas after 1990 display short-term fluctuations in ²⁰⁸Pb/²⁰⁶Pb on a time scale of 5-10 years (Marske et al., 2008; Greene et al., 2013). These isotopic variations are interpreted to result mostly from dynamic mantle processes. We postulated that these cycles in the Pb isotope ratios may result from the melting of a fine-scale repeating pattern of filament-shaped compositional heterogeneities (only ~1-3 km in diameter) in the mantle source region (Greene et al., 2013). Further Pb isotopic studies of post-2012 lavas are needed to evaluate the subsequent evolution of mantle source components and magma supply that contributed to the latter stages of this eruption.

Hypothetical parental magma compositions for the Pu'u 'Ō'ō magma were estimated (for discussion purposes) by normalizing lava compositions to 10 wt.% MgO (the highest MgO observed for the eruption). This was achieved by addition of equilibrium composition olivine and spinel in 0.5 mol.% steps with a mixture of 98.5% olivine and 1.5% spinel (as described by Garcia et al., 2003). We avoided three types of lava compositions for this procedure: 1. Those for episodes 1-31, 54 and 59 that formed by magma mixing. These samples are moderately fractionated (<7 wt.% MgO) and mixed with one or more components of older magma (Garcia et al., 1989; 1992; Walker et al., 2019). Also, many of these samples have undergone crustal contamination based on their relatively low δ^{18} O values compared to summit lavas (4.7-5.0% vs. >5.1-5.6%; Garcia et al., 1998, 2008). 2. Samples from 2012-2018 that have obvious geochemical signatures of gabbroic clots (CaO/TiO₂ >4.7; Fig. 4). 3. Other samples with MgO <7.0 wt.% that experienced clinopyroxene fractionation. The remaining 409 samples are thought to have only undergone fractionation of olivine with minor chromite.

The calculated parental magma compositions for Pu'u 'Ō'ō lava show remarkable and systematic long-term geochemical variations. Among the major elements, $CaO_{(10)}$ and $K_2O_{(10)}$ decline until day ~10,000 (Fig. 7). These oxides reversed their trend after day ~11,800 and increased until the end of the eruption on 01 May 2018 (day 12,903). The temporal trends for $TiO_{2(10)}$ (Fig. 4) and $P_2O_{5(10)}$ are generally similar to that of $K_2O_{(10)}$ (Greene et al. 2013), although TiO_2/K_2O progressively increases until day ~8000; afterwards it remains nearly constant before showing a sharp drop at day ~11,800 (Table S2). There was a small but progressive increase in

 $Al_2O_{3(10)}$ starting ~8000 day (Fig. 7). This trend has considerable scatter after day ~12,000 (Fig. 7), which may reflect the presence of sparse gabbroic clots with variable amounts of clinopyroxene and plagioclase that were not removed with our CaO/TiO₂ <4.7 filter.



The temporal trend of $SiO_{2(10)}$ shows a curious M-shaped trend starting around day 4000 with an increase until day ~6500 followed by a small decrease and a discontinuous increase at day ~9500. Afterwards, $SiO_{2(10)}$ decreases until the end of the eruption as $CaO_{(10)}$ and $K_2O_{(10)}$ increase (red samples in Fig. 7). Previous studies attributed the increase in $SiO_{2(10)}$ to the addition of magma from a mantle source component similar to that of Mauna Loa (Marske et al., 2008), following a suggestion by Pietruszka et al. (2006) based on $^{87}Sr/^{86}Sr$ and trace element ratios. This model is discussed in section 7 below.

Ratios of incompatible trace elements help to evaluate parental magma compositions. Such ratios avoid the effects of variable amounts of crystal fractionation or accumulation, and the presence of gabbroic clots. Key ratios for Hawaiian tholeilitic basalts include Nb/Y and La/Yb (e.g., Norman and Garcia, 1999; Pietruszka and Garcia, 1999a). These ratios in Pu'u 'Ō'ō lava show a systematic decline until day ~7000 (Figs. 4, 8). Afterwards, these ratios are relatively constant until day ~10,000 and then increase until the end of the eruption defining a broad U-shape trend (Fig. 8). The temporal pattern of decreasing Nb/Y and La/Yb corresponds to the tapping of recently depleted mantle within the Hawaiian plume (Pietruszka et al., 2006). The

subsequent increase in these ratios may indicate the supply of melt from a fresh mantle source (i.e., not previously melted beneath Hawai'i) and/or a decrease in the degree of mantle partial melting.

Perhaps surprisingly, the normalized major-element trends do not mimic the U-shaped patterns shown by the trace element ratios (Figs. 4, 7, 8), although the broad temporal pattern of increasing then decreasing $SiO_{2(10)}$ does approximate that of $^{87}Sr/^{86}Sr$ and the inverse of the trend for La/Yb. In addition, the overall positive correlation between $CaO_{(10)}$ and $K_2O_{(10)}$ with Th/Y (Fig. 9) suggests that some of the major element and trace element variations must reflect changes in the source composition and/or conditions of melting The overall change in MgO-normalized major elements and trace element ratios (especially the inflections in the temporal trends; Figs. 7 and 8) indicate significant changes in parental magma composition during the Pu'u 'Ō'ō eruption, possibly related to rapid changes in the deep structure of magma transport pathways that tap small scale mantle heterogeneities (e.g., Pietruszka et al., 2006).

An alternative model to explain the compositional variations at Pu'u 'Ō'ō posits variable mixing of compositionally distinct magmas within Kīlauea's plumbing system and no new mantle-derived parental magma (Thornber et al., 2015). This mixing is thought to have started in 2000 (~day 6200). The model advocates mixing of rift zone stored, magma (lower MgO) with higher MgO magma from the summit reservoir. This would explain the progressive but modest decrease in the MgO content in the erupted lava during the eruption as more magma with lower MgO was added. A simple test of this model utilizes the CaO/TiO₂. Rift zone stored magma has markedly lower CaO/TiO₂ (resulting from the fractional crystallization of clinopyroxene \pm plagioclase) than the higher MgO lava (<4.0 vs. >4.4) as shown by the lava from 1983, and episodes 54 and 59 (Fig. 9). However, the post-2000 erupted lava shows relatively constant CaO/TiO₂ (4.5 \pm 0.1) until 2011 (day ~10,000; Fig. 8) when gabbroic clots caused higher ratios. These results do not support this mixing model for the period from 2000-2010, prior to the episode 59 uprift eruption in 2011. Thus, it is our interpretation that multiple changes in the composition of the mantle-derived parental magmas occurred during the Pu'u 'Ō'ō eruption.

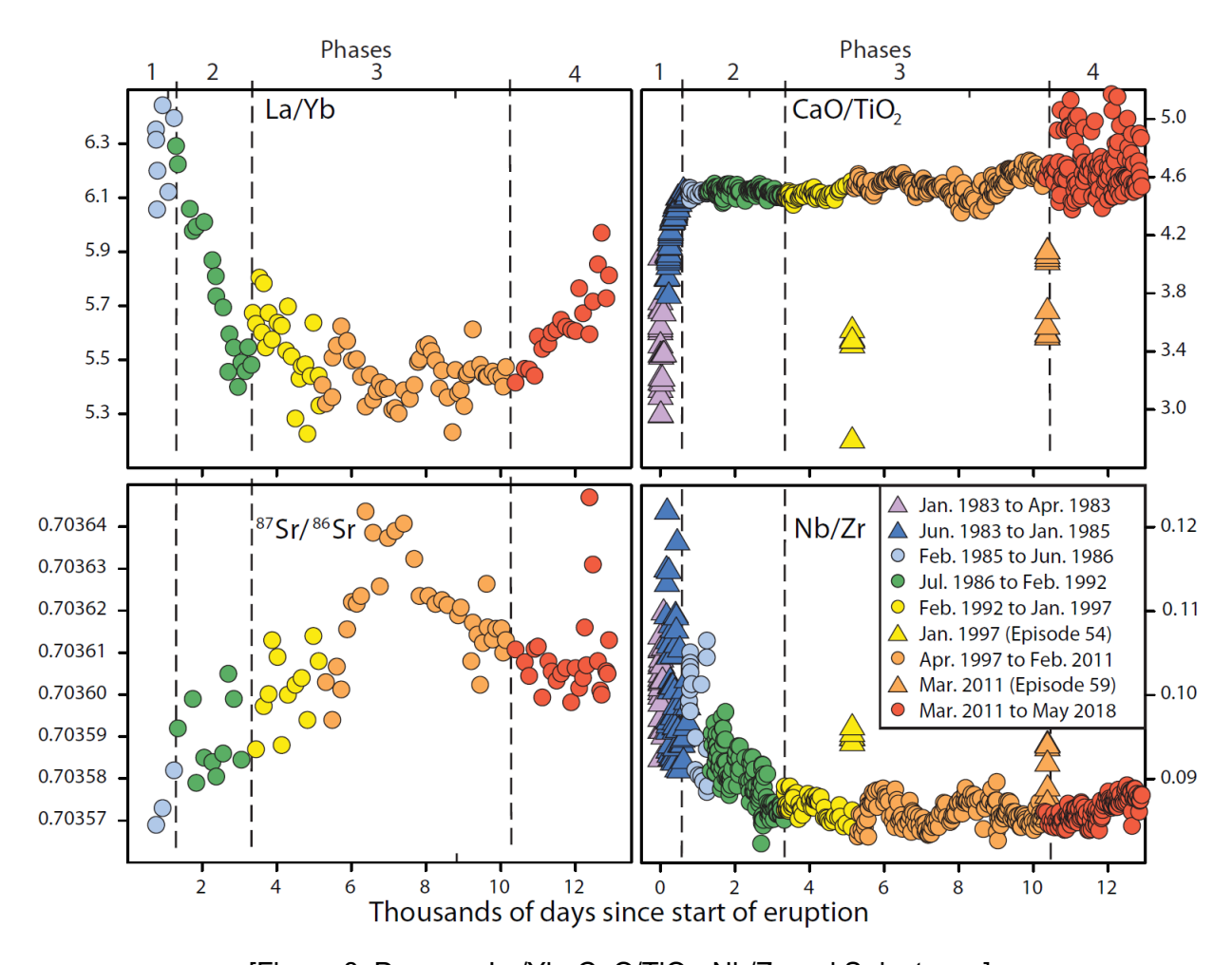
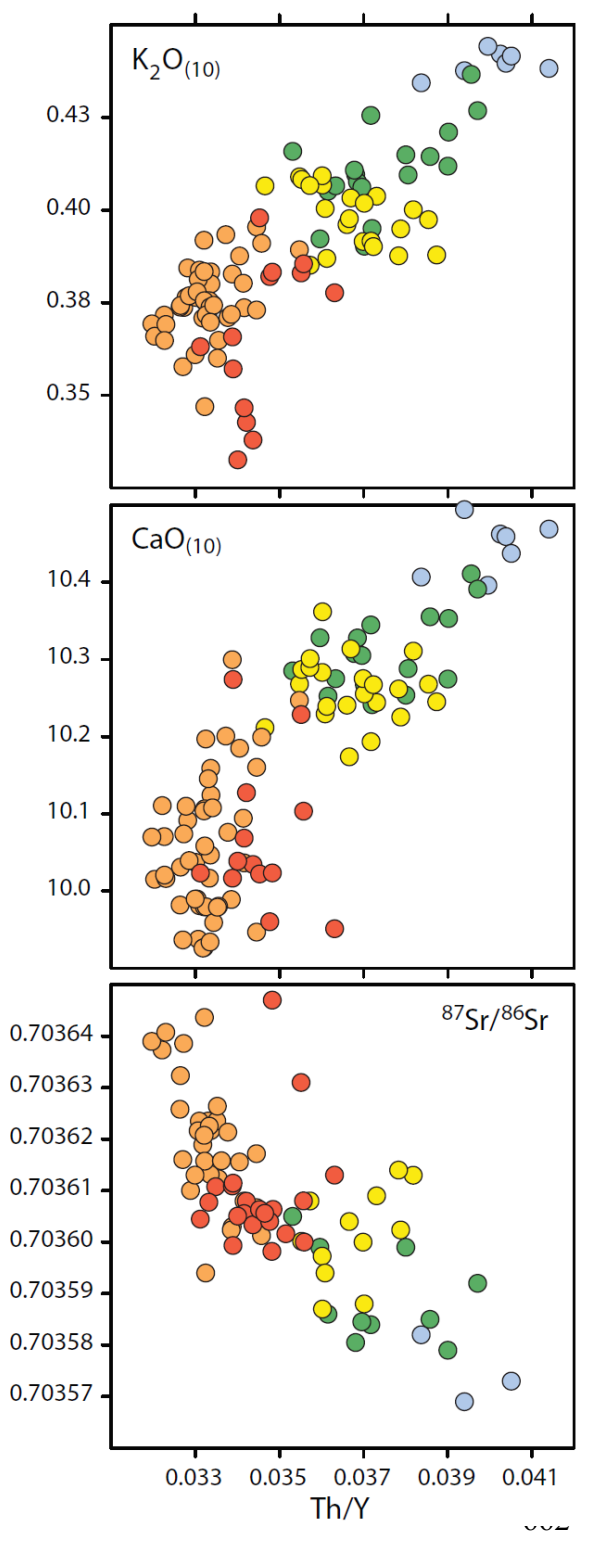


[Figure 8. Days vs. La/Yb, CaO/TiO₂, Nb/Zr and Sr isotopes]

7. Implications for Kīlauea's Source

Strontium isotope ratios provide insight into the variations of parental magma composition and the mantle source during the Pu'u 'Ō'ō eruption (Table 1; see Table S2 for a complete listing of all ⁸⁷Sr/⁸⁶Sr from our group). These ratios show an overall increase for the first ~7000 days of the eruption in harmony with the decrease in La/Yb (Fig. 8). Subsequently, there is a decrease in ⁸⁷Sr/⁸⁶Sr ratios with a correlated increase in La/Yb and Th/Y (Figs. 8 and 9). Near the end of the eruption, there is an abrupt shift to higher ⁸⁷Sr/⁸⁶Sr ratios for two samples (23-Nov-2016 and 24 Feb-2017; days 12,379, 12,472) followed by a rapid decrease to previous values (Fig. 8). The two late samples with higher ⁸⁷Sr/⁸⁶Sr and higher La/Yb are unlike the higher ⁸⁷Sr/⁸⁶Sr lavas erupted between days 6380-7683; (Fig. 8). Thus, they probably reflect a distinct source component.



663664

[Figure 9. Th/Y vs. $CaO_{(10)}$, and $K_2O_{(10)}$ and Sr isotopes]

The systematic changes in normalized major elements, trace element ratios and Sr isotope ratios (Figs. 6-8) require multiple source components and possible correlated variations in conditions (e.g., P-T-f) of melting. Historical (1790-1982) Kīlauea lavas also have large and systematic variations in Sr isotopic ratios, and a factor of 2 variation in degree of melting (Pietruszka and Garcia, 1999). Our early work on Pu'u 'Ō'ō lava suggested two Kīlauea-like source components were involved and that they were melted to increasing degrees based on a systematic decrease in incompatible elements and changes in Pb, Sr and Nd isotopes (Garcia et al., 2000). This model was refined using ²³⁰Th-²³⁸U and ²²⁶Ra-²³⁰Th disequilibria, incompatible trace element ratios (e.g., Th/U, Ba/Th, and Nd/Sm), and normalized major element abundances in lavas from 1985 to 2001 (Pietruszka et al., 2006). The models are consistent with 'recent depletion' (less than a few kyr) of a mantle source component by prior melting within the Hawaiian mantle plume (Pietruszka et al., 2006). This 'recently depleted'

component (with higher ⁸⁷Sr/⁸⁶Sr) was an increasingly important source for lavas erupted between 1985 and 1998.

Melt from a third mantle source component was delivered between 1998 and 2001 based on a small increase in the Ba/Th ratios of the lavas (Pietruszka et al., 2006) possibly reflecting involvement of a Mauna Loa-like mantle component (Pietruszka et al., 2006; Marske et al., 2008; Greene et al., 2013). Involvement of a Mauna Loa-like source is supported by the correlation of higher ⁸⁷Sr/⁸⁶Sr with high SiO₂₍₁₀₎ and low CaO₍₁₀₎ and K₂O₍₁₀₎ of Pu'u 'Ō'ō lavas from 1992 to 2007 (samples within the outlined field in Fig. 10). These features are characteristic of Mauna Loa (Rhodes et al., 1989; Rhodes and Hart, 1995). However, this interpretation appears to be inconsistent with the relatively constant Nb/Zr ratios of Pu'u 'Ō'ō lavas. Typically, Kilauea lavas have higher Nb/Zr ratios that those from Mauna Loa (>0.08 vs. <0.07; Rhodes et al., 1989). Although the Nb/Zr ratio of Pu'u 'Ō'ō lava varied from 0.82-0.11 during the eruption (Fig. 8), there was no discernible peak at day ~7000 as observed for ⁸⁷Sr/⁸⁶Sr and SiO₂₍₁₀₎ (Fig. 8). The Nb/Zr ratios of Pu'u 'Ō'ō lava are within the range of typical Kīlauea values.

Alternatively, the higher silica could represent a shallower depth of melting extraction based on experimental melting studies (see summaries by Longhi, 2002; Stolper et al., 2004; Putirka et al., 2011). This pressure dependence of the silica activity has been used to infer the depth of melt segregation (e.g., Albarède, 1992; Putirka, 2008; Lee et al., 2009). However, the use of silica activity to infer pressure of melt segregation is sensitive to: the presence of both olivine and orthopyroxene in the source; the mantle olivine composition (Fo91),;, the $K_{D(Fe-Mg)}$ between olivine and melt (0.34), and the oxidation state of the mantle at the time of melting (FMQ). Using the parameters listed above and following the methods of Lee et al. (2009), we infer pressures of ~3.1-3.5 GPa for the lower SiO_2 Pu'u 'Ō'ō lava (which are typical for Kilauea) and around 2.8 GPa for the higher SiO_2 lavas. These pressures correspond to melt segregation depths of ~115-130 km and ~95 km respectively (near the base of the lithosphere). These depth estimates may be somewhat shallow given that the lithosphere under Kīlauea is thought to be 100-100 km thick (Li et al., 2004).

Parental magma silica concentrations were also found to be variable in the Mauna Kea lavas in the Hawaii Scientific Project (HSDP) drill core. Higher and lower silica levels were reported in lavas that are otherwise geochemically similar (so-called Type-1 and Type-2 lavas; Rhodes and Vollinger, 2004). They have 48.7 vs. 47.5 wt.% SiO₂ at 13% MgO corresponding to inferred melt segregation depths of ~85 and 125 km. These lavas are inter-layered in the upper part of the HSDP core (depths of 353 to 1387 m). Apart from the differences in SiO₂, they have similar incompatible trace elements and isotopic ratios, implying a common source but differing depths of melt segregation. Garcia et al. (2007) estimated an average time interval between

Mauna Loa flows in the HSDP core of ~860 years. For the Puʻu ʻŌʻō eruption, the change in normalized silica (depth of melt segregation) occurred over ~2500 days (~7 years) from lower to higher $SiO_{2(10)}$ (49.5-50.2 wt.%) during Phase 3 (and even decreased and increased ~0.4 wt.% $SiO_{2(10)}$ again during Phase 3 before subsequently declining (Fig. 7). Thus, changes in the depth of melt segregation may occur more rapidly. Nonetheless, the isotopic variations of lava erupted during the Puʻu ʻŌʻō eruption require a heterogeneous source and not simply variable extents of melting of a homogeneous source.

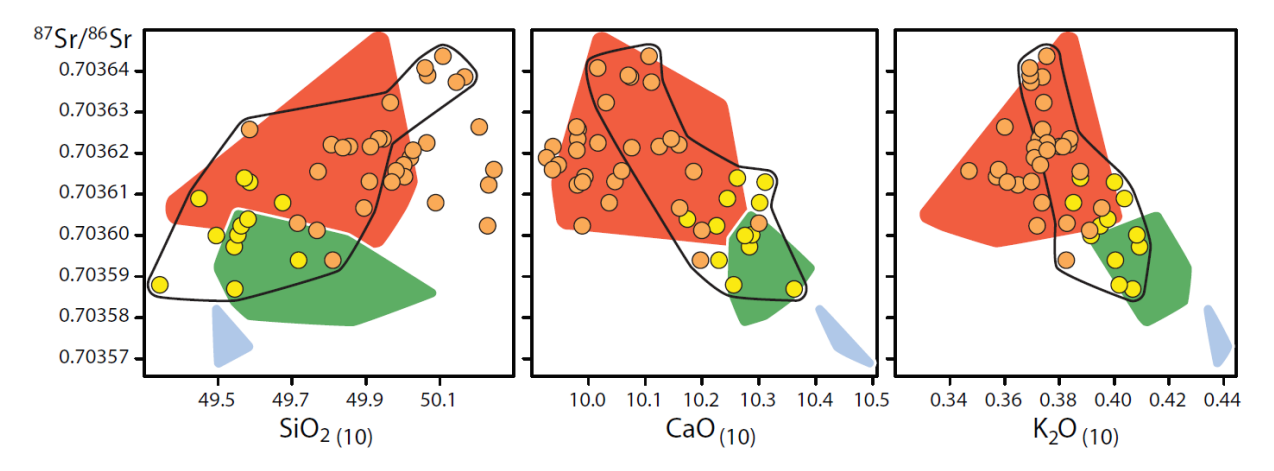


[Figure 10. Sr isotopes vs. normalized $CaO_{(10)}$, and $K_2O_{(10)}$]

The length scale of Kīlauea's mantle source heterogeneities must be relatively small to allow for rapid (few years) variation in lava ⁸⁷Sr/⁸⁶Sr values (Table 1). These source components may occur as blobs, pods, or filaments (Marske et al., 2007; Farnetani and Hofmann 2010; Greene et al., 2013). If the melting zone heights are ~5 km and the source heterogeneities are filaments, Greene et al. (2013) speculated that the filament diameter was ~3 km. Variable melt pathways may also play an important role in controlling the compositionally and isotopic variation produced during prolonged, voluminous eruptions like Pu'u 'Ō'ō (Pietruszka et al., 2001, 2006; Marske et al., 2008). At present, the relative importance of these two variables have not been quantified.

Finally, it is important to emphasize that the short-term geochemical fluctuations produced from Kīlauea's heterogeneous mantle source were effectively transported from the source to the surface over the last half century. Two factors played an important role in preserving these fluctuations: 1. Pu'u 'Ō'ō magmas are thought to either partially bypass the volcano's summit magma storage reservoir (Garcia et al., 2000) and/or the reservoir had minimal buffering capacity due to its small size (0.1-0.5 km³; Pietruszka et al., 2015); and 2. the high magma flux

rate during this eruption (~0.1 to >0.2 km³/year; Poland et al., 2012; Anderson and Poland, 2016).

8. Conclusions

The geochemical variations of lavas produced during the prolonged Pu'u 'Ō'ō eruption (1983 to 2018) illustrate the importance of time-series sampling to document the magmatic processes that can and do occur during an eruption. Our study of Pu'u 'Ō'ō lava geochemistry was initiated in 1983 to assist the USGS HVO staff in anticipating whether this would be a short-lived eruption (weeks to a few months) or might continue longer. When we determined the MgO content changed to higher MgO composition (>7.0 wt.% MgO) on day 161 of the eruption, it was a sign that this eruption might continue beyond the normal period of a few weeks or less. Little did we know back in 1983 that this eruption would become Kīlauea's longest-lived, and most voluminous historical magmatic event.

Sampling protocols (frequency and location) were modified as the eruption style changed from episodic with high lava fountains to continuous effusion. This was necessary as we realized the evolving scale (hours to months) of the compositional variations. Our systematic and extensive sampling, and thorough petrographic and geochemical analysis of the products of this eruption have demonstrated:

- Crustal processes (crystal fractionation, magma mixing, and crustal contamination)
 within Kīlauea's east rift zone are important. These processes play a key role in
 governing the compositional variations of lava at this volcano, especially for brief
 eruptions (days to weeks) as new summit magma is mixed with stored magma in the rift
 zone.
- 2. Voluminous and long-term eruptions like Pu'u 'Ō'ō allow magma to mostly overcome these crustal processes and permit the signatures of mantle-derived melts to be distinguished.
- 3. The parental magma composition of Pu'u 'Ō'ō lava varied substantially. There was a progressive decrease in incompatible element ratios for the first ~7000 days of the eruption followed by an increase for the last ~2500 days of the eruption. Overall, the trends of major and trace elements during the eruption are coupled and related to a changing parental magma.
- 4. Multiple mantle sources and possibly changes in melting conditions were involved in producing Pu'u 'Ō'ō parental magma. Three sources dominated the eruption with a possible fourth one at the end. These sources are Kīlauea-like with one having been

previously melted within the Hawaiian mantle plume to reduce its incompatible element content, without substantially modifying its isotopic character. A Mauna Loa-like source component may also have been involved but this requires additional research to confirm. Alternatively, the depth of melt segregation may have temporarily decreased during the middle part of the eruption.

Valuable lessons have been learned about mantle and crustal processes from this geochemical time-series analysis of lava from the Pu'u 'Ō'ō eruption. This study documented the interplay of magma storage (that resulted in crystal fractionation and crustal assimilation), and changing mantle sources and melting processes that affected the composition of the erupted lava during this long-lived eruption. Numerous questions remain regarding the causes of the remarkable geochemical variations during this eruption including: What are the relative roles of source composition vs. process (extent melting and/or depth of melting of melt extraction) in generating geochemical variation? Were any of these factors important for causing the long duration of this eruption? Was a Mauna Loa-like source involved in the Pu'u 'Ō'ō eruption? What is the nature and cause of the observed gabbro clots during Phase 4 of the eruption?

We strongly encourage others to systematically sample and rapidly analyze lava during future eruptions to assist eruption managers with gaining a better understanding of eruption processes, and to push forward our knowledge of magmatic processes.

Lastly, one purpose of this paper is to make the geoscience community aware of our extensive sample suite (>1300 samples; Table S1) and to invite those with a compelling and innovative project to request samples.

Acknowledgements.

This 38 year-long study would not have been possible without the support and assistance of many people and organizations. Samples for this study were collected by scores of people (see the Inventory Table S1 for a complete list). In particular, Scott Rowland, Cheryl Collamore, Zoe H. Thorne, Frank Trusdell, and John Hoffmann are thanked for collecting numerous samples. We also thank the Hawaiian Volcano Observatory staff for providing many of the samples we analyzed, especially from the first 3 years of the eruption, and for collaborating on various aspects of this study. In particular, we thank Ed Wolfe for inviting MG to assist at the start of the eruption with rapid analyzes, and Frank Trusdell, George Ulrich, Tim Orr for their collaboration with many aspects of this study including field work with MG. The XRF analyses reported here would not have been possible without the remarkable talents of Pete Dawson,

Michael Vollinger, Bart Martin, and Joel Sparks. The samples for this study were inventoried, crushed and powdered by numerous undergraduate students including Adonara Mucek, Kyle Tanguichi, John Hayes, Joann Romano, Chad Shishado and Nicole Robinson, Jocelyn Rayray, Jennifer Parker, R. Magu, Kelly Kolysko-Rose, and Ritchie Ho. Scott Rowland did an amazing job in assembling our flow field map (Figure 1). We thank Vickie Bennett for access to the RSES TIMS laboratory and advice on Sr isotopic measurements, and Sonja Zink for assistance with the Sr isotope chemistry, mass spectrometry, and data reduction. We thank the two journal reviewers, Dominique Weis and Francois Nauret, for their helpful comments on this paper. Funding for this long-term study was primarily from numerous National Science Foundation grants to MG. We greatly appreciate the trust that NSF program managers John Snyder, Sonia Esperance and Jennifer Wade gave us in providing grant funding for over 3 decades (most recently EAR-1449744). This is SOEST contribution number xxxxx.

Authors contribution

All of the authors participated in designing the study, were involved in collecting samples, contributed to the interpretation of the data, and in preparing the manuscript. MG was responsible for coordinating all aspects of this study including preparation of the manuscript, the sample descriptions, archiving, and the powdering the samples for chemical analyzes. JMR oversaw the XRF analyses. AP assisted in compiling the published ICPMS trace element and Sr isotope analyzes, and drafted figures 4-10 for this paper. MN contributed the new ICPMS trace element and Sr isotope data presented in the manuscript.

Declaration of Competing Interest

The authors declare that they have no known competing financial interests or personal relationships that would have influenced the work reported in this paper.

References

- Albarède, F., 1992. How deep do common basaltic magmas form and differentiate? J. Geophys. Res. 97, 10,997-11,009.
- Albarède, F., 1996. High-resolution geochemical stratigraphy of Mauna Kea flows from the Hawaii Scientific Drilling Project core. J. Geophys. Res. 101, 11841-11853.
- Albarède, F., Tamagnan, V., 1988. Modelling the recent geochemical evolution of the Piton de la Fournaise Volcano, Réunion Island, 1931-1986. J. Petrol. 29, 997-1030.
 - Albarède, F., Luais, B., Fitton, G., Semet, M., Kaminski, E., Upton, B.G.J., Bachèlery, P., Cheminée, J.-L., 1997. The geochemical regimes of Piton de la Fournaise Volcano (Réunion) during the last 530,000 years. J. Petrol. 38, 171-201.
 - Anderson, K.R., Poland, M.P., Johnson, J.H., Miklius, A., 2015. Episodic deflation-inflation events at Kīlauea Volcano and implications for the shallow magma system," in Hawaiian Volcanism: From Source to Surface, Eds. Carey, R.J., Poland, M.P., Cayol, V., Weis, D., Eds. AGU Geophys. Mono. Series 208, AGU, pp. 229–250; DOI: 10.1002/9781118872079.ch11.
 - Anderson, K.R., Poland, M.P., 2012. Bayesian estimation of magma supply, storage, and eruption rates using a multiphysical volcano model: Kilauea Volcano, 2000–2012. Earth Planet. Sci. Lett. 447, 161–171.
 - Anderson, K.R., Johanson, I.A., Patrick, M.R., Gu, M., Segall, P., Poland, M.P., Montgomery-Brown, E.K. and Miklius, A., 2019. Magma reservoir failure and the onset of caldera collapse at Kilauea Volcano in 2018. Science 266, DOI:10.1126/science.aaz1822.
 - Blichert-Toft, J., Weis, D. Maerschalk, C., Albarede, F., 2003. Hawaiian hotspot dynamics as inferred from the Hf and Pb isotopic evolution of Mauna Kea volcano. Geochem. Geophys. Geosyst. 4, 2002GC000340.
 - Bryce, J.G., DePaolo, D.J., Lassiter, J.C., 2005. Geochemical structure of the Hawaiian plume: Sr, Nd, and Os isotopes in the 2.8 km HSDP-2 section of Mauna Kea volcano. Geochem. Geophys. Geosyst. 6:Q09G18. doi:10.1029/2004GC000809.
 - Caroff, M., Maury, R.C., Vidal, P., Guille, G., Dupuy, C., Cotten, J., Guillou, H., Gillot, P.-Y., 1995. Rapid Temporal Changes in Ocean Island Basalt Composition: Evidence from an 800 m Deep Drill Hole in Eiao Shield (Marquesas), J. Petrol. 36, 1333-1365, https://doi.org/10.1093/petrology/36.5.1333.
 - Deniel, C., Pin, C., 2001. Single-stage method for the simultaneous isolation of lead and strontium from silicate samples for isotopic measurements. Anal. Chim. Acta 426, 95-103.
 - DePaolo, D. J., Stolper, E. M., 1996. Models of Hawaiian volcano growth and plume structure: implications of results from the Hawaii Scientific Drilling Project. J. Geophys. Res. 101, 11643-11654.
 - Dzurisin, D., Koyanagi, R.Y., English, T. T., 1984. Magma supply and storage at Kīlauea Volcano, Hawai'i 1956-1983. J. Volcanol. Geotherm. Res. 21, 177-206.
 - Eggins, S.M., Woodhead, J.D.. Kinsley, L.P.J., Mortimer, G.E., Sylvester, P., McCulloch, M.T., Hergt, J.M., Handler, M.R., 1997. A simple method for the precise determination of > 40 trace elements in geological samples by ICPMS using enriched isotope internal standardisation. Chem. Geol. 134, 311-326.
- Farnetani, C.G., Hofmann, A.W., 2010. Dynamics and internal structure of the Hawaiian plume. Earth Planet. Sci. Lett. doi:10.1016/j.epsl.2010.04.005.
- Gansecki, C., Lee, R.L., Shea, T., Lundblad, S.P., Hon, K., Parcheta C., 2019. The tangled tale of Kīlauea's 2018 eruption as told by geochemical monitoring. Sci. 366, eaaz0147. https://doi.org/10.1126/science.aaz0147.
- Garcia, M. O., 2015. How and why Hawaiian volcanism has become pivotal to our understanding of volcanoes from their source to the surface. In: Carey, R. J., Cayol, V.,

- Poland, M. P. & Weis, D. (eds.) Hawaiian Volcanoes: From Source to Surface. American Geophysical Union, Geophysical Monograph 208, 1-18.
- Garcia, M.O., 1996. Petrography and olivine and glass chemistry of lavas from the Hawaii Scientific Drilling Project. J. Geophys. Res. 101, 11,701-11,713.
- Garcia, M.O., Wolfe, E.W., 1988. Petrology of the erupted lava. U.S. Geol. Surv. Prof. Paper 1463, 127-143.
- Garcia, M.O., Ho, R., Rhodes, J.M., Wolfe, E., 1989. Petrologic constraints on rift zone processes: Results from episode 1 of the Puu Oo eruption of Kīlauea Volcano, Hawaii. Bull. Volcanol. 52, 81-96.
 - Garcia, M.O., Rhodes, J.M., Ho, R., Wolfe, E.W., Ulrich, G.E., 1992. Petrology of lavas from episodes 2-47 of the Puu Oo eruption of Kīlauea Volcano, Hawaii: Implications for magmatic processes. Bull. Volcanol. 55, 1-16.
 - Garcia, M.O., Rhodes, J.M., Trusdell, F.A., Pietruszka, A., 1996. Petrology of lavas from the Puu Oo eruption of Kīlauea Volcano: III. The Kupaianaha episode (1986-1992). Bull. Volcanol. 58, 359-379.
 - Garcia, M.O., Ito, E., Eiler, J., Pietruszka, A., 1998. Crustal contamination of Kīlauea Volcano magmas revealed by oxygen isotope analysis of glass and olivine from the Puu Oo eruption lavas. J. Petrol. 39, 803-817.
 - Garcia, M.O., Pietruszka, A.J., Rhodes, J.M., Swanson, K., 2000. Magmatic processes during the prolonged Puu Oo eruption of Kīlauea Volcano, Hawaii. J. Petrol. 41, 967-990.
 - Garcia, M.O., Pietruszka, A.J., Rhodes, J.M., 2003. A petrologic perspective of Kīlauea Volcano's summit magma reservoir. J. Petrol. 44, 2313-2339.
 - Garcia, M.O., Haskins, E.H., Stolper, E., Baker, M., 2007. Stratigraphy of the Hawaiian Scientific Drilling Project: Anatomy of a Hawaiian volcano. Geochem., Geophys., Geosyst. 8, Q02G20, doi:10.1029/2006GC001379.
 - Garcia, M.O., Ito, E. and Eiler, J.M., 2008. Oxygen isotope evidence for chemical interaction of Kīlauea historical magmas with basement blocks. J. Petrol. 49, 757-769.
 - Garcia, M.O., Jicha, B.R., Marske, J.P., Pietruszka, A.J., 2017. How old is Kīlauea Volcano? Insights from ⁴⁰Ar/³⁹Ar dating of the 1.7-km-deep SOH-1 core. Geology, 45, 79-82, doi:10.1130/G38419.1.
 - Greene, A., Garcia, M.O., Pietruszka, A., Weis, D., Marske, J., Maerschalk, C., Vollinger, M.J., Eiler, J., 2013. Temporal geochemical variations in lavas from Kīlauea's Pu'u 'Ō'ō eruption (1983-2010): Cyclic variations of Pb isotope ratios from the melting of vertical source heterogeneities. Geochem., Geophys., Geosyst. 14, 11, doi: 10.1002/2013GC004719.
 - Harris, A.J.L., Keszthelyi, L., Flynn, L.P., Mouginis-Mark, P.J., Thornber, C., Kauahikaua, J., Sherrod, D., Trusdell, F., Sawyer, M.W., Flament, P., 1997. Chronology of the episode 54 eruption at Kīlauea Volcano, Hawaii, from GOES-9 satellite data. Geophys. Res. Letts. 24, 3281-3284.
 - Heliker, C., Mangan, M.T., Mattox, T.N., Kauahikaua, J.P., Helz, R. T., 1998. The character of long-term eruptions: inferences from episodes 50-53 of the Puu Oo-Kupaianaha eruption of Kīlauea Volcano. Bull. Volcanol. 59, 381-393.
- Heliker C.C., Mattox T.N., 2003. The first two decades of the Pu'u 'O'o-Kupaianaha eruption: Chronology and selected bibliography. U.S. Geol. Surv. Prof. Paper 1676: 1-28.
- Heliker, C., Swanson, D.A., Takahashi, T.J., 2003. The Puu Oo-Kupaianaha Eruption of Kīlauea Volcano, Hawaii: the First 20 Years. U.S. Geol. Surv. Prof. Paper 1676, 206 p.
- 911 Helz, R.T., Thornber, C.R., 1987. Geothermometry of Kīlauea Iki lava lake, Hawaii. Bull. 912 Volcanol. 49, 651-668.
- Hoffmann, J.P., Ulrich, G.E., Garcia, M.O. 1990. Horizontal ground deformation patterns and magma storage during the Puu Oo eruption of Kīlauea volcano, Hawaii: episodes 22-42. Bull.

915 Volcanol. 52, 522-531.

- Hofmann, A.W., Feigenson, M.D., Raczek, I., 1984. Case studies on the origin of basalt: III.
 Petrogenesis of the Mauna Ulu eruption, Kīlauea, 1969-1971. Contrib. Mineral. Petrol. 88,
 24-35.
- Holcomb, R., 1987. Eruptive history and long-term behavior of Kīlauea Volcano. U.S. Geol.
 Surv. Prof. Paper 1350, 261-350. Lee, C.-T., Luffi, P., Plank, T., Dalton, H., Leeman, W.P.,
 2009. Constraints on the depth and temperatures of basaltic magma generation on Earth and other terrestrial planets using a new barometer for mafic magmas. Earth Planet. Sci.
 Lett. 279, 20-33.
- Li, X., Kind, R., Yuan, X., Wölbern, I., Hanka, W., 2004. Rejuvenation of the lithosphere by the Hawaiian plume. Nature 427, 827–829.
 - Longhi, J., 2002. Some phase equilibrium systematics of Iherzolite melting. Geochem. Geophys. Geosyst., 1020, doi10,1029/2001GC000204.
- Macdonald, G.A., Abbott, A.T., Peterson, F.L., 1983. Volcanoes in the Sea. University of Hawaii Press, Honolulu, 89-81.
 - Marske, J.P., Pietruszka, A.J., Weis, D. Garcia, M.O., Rhodes, J.M., 2007. Rapid passage of a small-scale mantle heterogeneity through the melting regions of Kīlauea and Mauna Loa Volcanoes, Hawai'i. Earth Planet. Sci. Lett. 259, 34-50.
 - Marske, J.P., Garcia, M.O., Pietruszka, A.P., Rhodes, J.M., Norman, M.D., 2008. Geochemical variations during Kīlauea's Puu Oo eruption reveal a fine-scale mixture of mantle heterogeneities within the Hawaiian plume. J. Petrol. 49, 1297-1318.
 - Mittelstaedt, E., Garcia, M. O., 2007. Modeling the sharp compositional interface in the Pu`u `Ō`ō magma reservoir, Kīlauea volcano, Hawaii. Geochem. Geophys. Geosyst. 8, Q05011, doi:10.1029/2006GC001519.
 - Montgomery-Brown, E., Sinnett, D., Poland, M., Segall, P., Orr, T., Zebker, H., Miklius, A., 2010. Geodetic evidence for en echelon dike emplacement and concurrent slow-slip during the June 2007 intrusion and eruption at Kilauea Volcano, Hawai'i, *J. Geophys. Res.*, 115, B07405, doi:10.1029/2009JB006658.
 - Moore, R.B., Helz, R.T., Dzurisin, D., Eaton, G.P., Koyanagi, R.Y., Lipman, P.W., Lockwood, J.P., Puniwai, G.S., 1980. The 1977 eruption of Kılauea Volcano, Hawai'i. J. Volcanol. Geotherm. Res. 7, 189–210.
- 946 Neal, C. A., Brantley, S.R., Antolik L., Babb, J.L., Burgess M., Calles, K., Cappos, M., Chang, 947 J.C., Conway, S., Desmither, L., Dotray, P., Elias, T., Fukunaga, P., Fuke, S., Johanson, 948 I.A., Kamibayashi, K., Kauahikaua, J., Lee, R.L., Pekalib, S., Miklius, A., Million, W., Moniz, 949 C.J., Nadeau, P.A., Okubo, P., Parcheta, C., Patrick, M.P., Shiro, B., Swanson, D.A., Tollett, 950 W., Trusdell, F., Younger, E.F., Zoeller, M.H., Montgomery-Brown, E.K., Anderson, K.R., 951 Poland, M.P., Ball, J.L., Bard, J., Coombs, M., Dietterich, H. R., Kern, C., Thelen, W.A., 952 Cervelli, P.F., Orr, T., Houghton, B.F., Gansecki, C., Hazlett, R., Lundgren, P., Diefenbach, 953 A.K., Lerner, A.H., Waite, G., Kelly, P., Clor, L., Werner, C., Mulliken, K., Fisher, G., Damby, 954 D., 2018. The 2018 rift eruption and summit collapse of Kīlauea Volcano. Science 363, 367-955 374, https://doi.org/10.1126/science.aav7046.
 - Nobre-Silva, Inês G., Weis, D., Scoates, J.S., Barling, J., 2013. The Ninetyeast Ridge and its Rrelation to the Kerguelen, Amsterdam and St. Paul hotspots in the Indian Ocean, J. Petro. 54, 1177–1210, https://doi.org/10.1093/petrology/egt009.
- Norman M.D., Garcia M. O., Bennett V. C., 2004. Rhenium and chalcophile elements in basaltic glasses from Ko'olau and Moloka'i volcanoes: Magmatic outgassing and composition of the Hawaiian plume. Geochim. Cosmochim. Acta 68, 3761-3777.
- Orr, T.R., Poland, M.P., Patrick, M.R., Thelen, W.A., Sutton, A.J., Elias, T., Thornber, C.R.,
 Parcheta, C., Wooten, K.M., 2015. Kīlauea's 5-9 March 2011 Kamoamoa fissure eruption
 and its relation to 30+ years of activity from Pu'u 'Ō'ō. In: Carey, R. J., Cayol, V., Poland, M.
 P. & Weis, D. (eds.) Hawaiian Volcanoes: From Source to Surface, Am. Geophys. Un.

966 Geophys. Mono. 208, 393-420.

926

927

930

931

932

933

934

935

936

937

938

939

940

941

942

943

944

945

956

957

- Patrick, M.R., Anderson, K.R., Poland, M.P., Orr, T.R., Swanson, D.A., 2015. Lava lake level as a gauge of magma reservoir pressure and eruptive hazard. Geology 43, 831–834, doi: 10.1130/G36896.1.
- Patrick, M.R., Orr, T., Sutton, A.J., Elias, T., Swanson, D., 2013, The first five years of Kīlauea's summit eruption in Halema'uma'u Crater, 2008–2013: U.S. Geol. Surv. Fact Sheet 2013-3116, 4 p.
- Pietruszka, A.P., Garcia, M.O., 1999. A rapid fluctuation in the mantle source and melting
 history of Kīlauea Volcano inferred from the geochemistry of it historical summit lavas (1790 J. Petrol. 40, 1321-1342.
- 976 Pietruszka, A.P., Rubin, K.H., Garcia, M.O., 2001. ²²⁶Ra-²³⁰Th-²³⁸U disequilibria of historical Kilauea lavas (1790-1982) and the dynamics of mantle melting within the Hawaiian plume. Earth Planet. Sc. Lett. 186, 15-31.
 - Pietruszka, A.J., Hauri, E.H., Carlson, R.W., Garcia, M.O., 2006. Remelting of recently depleted mantle within the Hawaiian plume inferred from the ²²⁶Ra-²³⁰Th-²³⁸U disequilibria of Pu'u 'Ō'ō eruption lavas. Earth Planet. Sci. Letts. 244, 155–169.
 - Pietruszka, A.J., Heaton, D.E., Marske, J.P., Garcia, M.O., 2015. Two magma bodies beneath the summit of Kīlauea Volcano unveiled by isotopically distinct melt deliveries from the mantle. Earth Planet. Sci. Lett. 413, 90-100.
 - Pietruszka, A.J., Marske, J.P., Garcia, M.O., Heaton, D.E., Rhodes, J.M., 2018. An isotopic perspective into the magmatic evolution and architecture of the rift zones of Kīlauea Volcano. J. Petrol. 59, 2311–2352, doi: 10.1093/petrology/egy098.
 - Pietruszka, A.J., Marske, J.P., Garcia, M.O., Heaton, D.E., Rhodes, J.M., 2021. Accumulated Pu'u 'Ō'ō magma fed the voluminous 2018 rift eruption of Kīlauea Volcano: Evidence from lava chemistry. Bull. Volc., in review.
 - Poland, M. P., 2014. Time-averaged discharge rate of subaerial lava at Kīlauea Volcano, Hawai'i, measured from TanDEM-X interferometry: Implications for magma supply and storage during 2011–2013. J. Geophys. Res. Solid Earth 119, 5464–5481, doi:10.1002/2014JB011132.
 - Poland, M.P., Miklius, A., Sutton, A.J., Thornber, C.R., 2012. A mantle-driven surge in magma supply to Kīlauea Volcano during 2003-2007. Nature Geosci. 5, 295-300.
 - Poland, M.P., Miklius, A., Montgomery-Brown, E.K., 2014. Magma supply, storage, and transport at shield-stage Hawaiian volcanoes. In: Poland, M.P., Takahashi, T.J. and Landowski, C.M. (eds.), Characteristics of Hawaiian Volcanoes, U.S. Geol. Surv. Prof. Paper 1801, 179-234.
 - Putirka, K.D. 2008. Thermometers and barometers for volcanic systems. In: Putirka, K.D. and Tepley III, F. J. (eds.), Minerals, Inclusions and Volcanic Processes, Reviews in Mineralogy and Geochemistry 69, 61-120.
- Quane, S.L., Garcia, M.O., Guillou, H., Hulsebosch, T.P., 2000. Magmatic history of the east rift zone of Kilauea Volcano, Hawaii based on drill core from SOH1. J. Volcanol. and Geotherm. Res. 102, 319-338.
- Rhodes, J.M., 1988. Geochemistry of the 1984 Mauna Loa eruption: Implications for magma storage and supply. J. Geophys. Res. 93, 4453-4466.
- Rhodes, J. M., 1996. The geochemical stratigraphy of lava flows sampled by the Hawaii Scientific Drilling Project. J. Geophys. Res. 101, 11,729-11,746.
- Rhodes, J.M., Wenz, K.P., Neal, C. A., Sparks, J.W., Lockwood, J. P., 1989. Geochemical evidence for the invasion of Kilauea's magmatic plumbing system by Mauna Loa magma, *Nature*, *337*, 257-360.
- Rhodes, J.M., Hart, S.R., 1995. Episodic trace element and isotopic variations in historical Mauna Loa lavas: implications for magma and plume dynamics. Am. Geophys. Un.
- 1016 Geophys. Mono. 92, 263-286.

979

980 981

982

983

984

985

986

987

988

989

990

991

992

993

994

995

996

997

998

999

1000

1001

1002

- Rhodes, J.M., Vollinger, M.J., 2004. Compositions of basaltic lavas sampled by phase-2 of the Hawaiian Scientific Drilling Project: Geochemical stratigraphy and magma types: Geochem. Geophys. Geosyst. 5, Q03G13, doi:10.1029/2002GC000434.
- Rhodes, J.M., Huang, S., Frey, F.A., Pringle M., Xu, G., 2012. Geochemical evidence for the invasion of compositional diversity of lavas recovered by the Hawaii Scientific Drilling Project: Has the core sampled lavas from multiple volcanoes and from both peridotite and pyroxenite sources?, Geochem. Geophys. Geosyst. 13. QO3014 doi:10
- Shamberger, P.J., Garcia, M. O., 2007. Geochemical modeling of magma mixing and magma reservoir volumes during early Pu'u 'O'o eruption of Kīlauea Volcano. Bull. Volcanol. 69, 345-352.
- Sutton, J.A., Elias,T., Kauahikaua, J., 2003. Lava-effusion rates for the Puu Oo-Kupaianaha eruption derived from SO2 emissions and very low frequency (VLF) measurements. In: Heliker, C., Swanson, D.A., Takahashi, T.J. (Eds.) The Puu Oo-Kupaianaha Eruption of Kīlauea Volcano, Hawaii: the First 20 Years. U.S. Geol. Surv. Prof. Paper 1676, 121-136.
- Thornber, C.R., 2001. Olivine-liquid relations of lava erupted by Kīlauea volcano from 1994 to 1998: implications for shallow magmatic processes associated with the ongoing East-Rift-Zone eruption. Canad. Mineral. 39, 239-266.
- Thornber, C.R., 2003. Magma-reservoir processes revealed by geochemistry of the Puu Oo-Kupaianaha eruption. In: Heliker, C., Swanson, D. A., Takahashi, T. J. (Eds.), The Puu Oo-Kupaianaha Eruption of Kīlauea Volcano, Hawaii: the First 20 Years. U.S. Geol. Surv. Prof. Paper 1676, 121-136.
- Thornber, C.R., Heliker, C., Sherrod, D.R., Kauahikaua, J.P., Miklius, A., Okubo, P.G., Trusdell, F. A., Budahn, J. R., Ridley, W. I., Meeker, G. P., 2003. Kīlauea east rift zone magmatism; an episode 54 perspective. J. Petrol. 44, 1525-1559.
- Thornber, C.R., Orr, T.R., Heliker, C., Hoblitt, R.P., 2015. Petrologic testament to changes in shallow magma storage and transport during 30+ years of recharge and eruption at Kīlauea Volcano, Hawaiʻi. In: Carey, R.J., Cayol, V., Poland, M.P., Weis, D. (eds.) Hawaiian Volcanoes: From Source to Surface, Am. Geophys. Un. Geophys. Mono. 208, 147-188.
- Tilling, R.I., Dvorak, J.J., 1993. Anatomy of a basaltic volcano. Nature 363, 125-133.
- Vlastélic, I., Deniel, C., Bosq, C., Télouk, P., Boivin, P., Bachèlery, P., Famin, V., Staudacher,
 T., 2009. Pb isotope geochemistry of Piton de la Fournaise historical lavas. Journal.
 Volcanol. Geotherm. Res. 184, 63-78.
- Walker, B., Garcia, M.O. Orr, T.R., 2019. Petrologic Insights into Rift Zone Magmatic Interactions under Kilauea's Napau Crater (1922-2011), J. Petrol. 60, 2051–2075.

1054

- Watson, S., McKenzie, D., 1991. Melt generation by plumes: A study of Hawaiian volcanism. J.
 Petrol. 32, 501-537.
 Weis, D., Garcia, M.O., Rhodes, J.M., Jellinek, M., Scoates, J.S., 2011. Role of the deep mantle
 - Weis, D., Garcia, M.O., Rhodes, J.M., Jellinek, M., Scoates, J.S., 2011. Role of the deep mantle in generating the compositional asymmetry of the Hawaiian mantle plume. Nature Geosci. 4, 831-838.
- Wolfe, E., Garcia, M.O., 5 others, 1987. The Puu O'o eruption of Kīlauea Volcano, episodes 1-20. U.S. Geol. Surv. Prof. Paper 1350, 471-508.
- Wolfe, E.W., Neal, C.A., Banks, N.G., Duggan, T.J., 1988 Geologic observations and chronology of eruptive events. U.S. Geol. Surv. Prof. Paper 1463, 1-97.
- Wright, T.L., 1971. Chemistry of Kīlauea and Mauna Loa lavas in space and time. U.S. Geol. Surv. Prof. Paper 735, 1-45.
- Wright, T.L., Fiske, R.S., 1971. Origin of the differentiated and hybrid lavas of Kīlauea Volcano, Hawaii. J. Petrol. 12, 1-65.
- Wright, T.L., Tilling, R.I., 1980. Chemical variations in Kilauea eruptions 1971–1974, In: Irving, A.J., Dungan, M.A., (eds.), Am. J. Sci. 280-A, 777–793.
- Wright, T.L., Klein, F.W., 2006. Deep magma transport at Kīlauea Volcano, Hawaii. Lithos 87, 50-79.

Figure captions

Figure 1. Map of the southeast flank of the Island of Hawai'i showing the Pu'u 'Ō'ō lava flow field overlain on a DEM image. The four phases of the eruption are color coded. Almost all of the lava from Phase 1 (light blue) is covered by lava from subsequent phases. The two main vents for the eruption are labeled (Pu'u 'Ō'ō and Kupaianaha). The location of the lava lake that was active from 2008-2018 at the summit of Kīlauea in Halema'uma'u crater is shown in orange. Black lines are roads.

10741075

1076

1077

1078

1079

1080

1081

1082

1083

1084

1085

1086

1087

1088

1089

1090

1091

1092

1093

1094

1068

1069

1070

1071

1072

1073

Figure 2. Interpretative cross section of Kīlauea volcano from the summit area (site of Halema'uma'u crater) east along the axis of the east rift zone to where the Pu'u 'Ō'ō eruption was focused in the rift's middle section. The cross section is based on surface vent locations, the geochemistry of the eruptive lavas (Garcia et al., 1989; 1992; 1996, 2000; Marske et al., 2008; Greene et al., 2013) and prior knowledge of the magmatic plumbing system of Kīlauea (e.g., Poland et al., 2014). Kīlauea is fed from the mantle via a primary conduit underlying the summit area. a) Eruptions from 1977 to April 1983. Pre-Pu'u 'Ō'ō eruptions occurred at the summit in 1982 and at multiple sites along the upper (Nov. 1979 and Mar. 1980) and middle east rift zone (1977). The east rift zone eruptions involved magmas stored for decades before the eruption (shown in yellow; Pietruszka et al. 2019). The early Pu'u 'Ō'ō eruptions (January-April 1983, episodes 1-3) involved mixing of two pockets of magma stored in the rift zone (yellow and orange) and eruption from multiple fissures. In June 1983, this hybrid was mixed with hotter, more MgO-rich magma intruded from the summit (Garcia et al., 1989; 1992). b) The eruption localized at the Pu'u 'Ō'ō vent during episode 4. A satellite vent, Kupaianaha, was the primary locus of activity during Phase 2 from 1986-1992 (episode 48, Garcia et al., 1996). The primary site of effusion returned to Pu'u 'Ō'ō in 1992 for Phases 3 and 5 of the eruption. Effusion also occurred to 2-4 km west of the Pu'u 'Ō'ō vent in 1997 and 2011 in the same area as the earlier Pu'u 'Ō'ō fissure eruptions. A third, brief (hours) eruption occurred 6 km west of Pu'u 'Ō'ō in 2007.

10951096

1097

1098

1099

1100

1101

Figure 3. Photomicrographs of Pu'u 'Ō'ō lavas. Images A, B and D were taken in plain polarized light with crossed nicols. Image C was taken without crossed nicols. The scale for images A, B and C are as shown in image A. Image D used lower magnification. A. Sample KE31-367 (day 801) with sparse, small (usually <1 mm) olivine (ol) with very small chromite inclusions (ch; black squares) in a glassy matrix. B. Sample 25 Sep 1988 (day 2093) with abundant small, euhedral olivine in a glassy matrix. C. Sample KE3-88 (day 85) with common clinopyroxenes

(cpx) and some plagioclases (plag) in a brown, glassy matrix. D. Sample 21 Sep 2016 (day 12,316) with gabbroic clots (primarily clinopyroxene with plagioclase and rare magnetite), a common feature of Phase 4 samples.

Figure 4. MgO variation diagram for lavas from the Puʻu ʻŌʻō eruption based on XRF analyzes. The eruption is subdivided and color coded into time segments reflecting the different time and areas of eruption. Phase 1 (purple and blues) includes Jan. 1983-June 1986. Phase 2 (green) is Jul. 1986-Feb. 1992. Phase 3 (yellow and orange) is Feb. 1992-Mar. 2011. Phase 4 (red) is Mar. 2011-May. 2018. Triangles are for the evolved and mixed samples from episodes 1-30, 54 and 59. Circles are for the less evolved samples. The kinks in the CaO and Al_2O_3 plots are related to crystallization of clinopyroxene and plagioclase respectively. The red circles with high CaO/TiO_2 (>4.7) have gabbroic clots. The TiO_2 plot shows an overall curved trend reflecting the absence of a Ti-rich mineral in the Puʻu ʻŌʻō crystallization sequence. Note the progressive decrease in TiO_2 with time.

Figure 5. Plot of Cr vs. Nb and Ni contents based on XRF analyzes of Pu'u 'Ō'ō lava color coded for temporal variation (see Figure 3 for color time periods). Note the different trends for the different time periods. Overall, Nb and Ni decreased for a given Cr content with time.

Figure 6. Temporal variation of MgO, CaO/Al₂O₃ and Nb/Y based on XRF analyzes for Pu'u 'Ō'ō lava. The evolved and mixed lavas generally have lower MgO and CaO/Al₂O₃ and higher Nb/Y that the other lava. Note the overall progressive trends in the MgO and ratios with time until about day 10,000. The wide ranges in MgO reflect variations in the magma supply rate and eruption (see the next for details on these processes). Samples from episodes 54 and 59 (triangles) plot outside the trends for the other higher MgO samples. See Figure 3 for the symbol legend.

Figure 7. Temporal variation of normalized values to 10 wt.% for MgO for SiO₂, CaO, Al₂O₃ and K₂O in Pu'u 'Ō'ō lava (see Figure 3 for color time periods). See text for description of the normalization procedures, and for which samples were excluded from this procedure. $CaO_{(10)}$ and K₂O₍₁₀₎ show progressive decreasing trends until about day 11,500 during the eruption and then an increase, whereas Al₂O₃₍₁₀₎ shows a broad increasing trend but with lots of scatter after day 11,500 probably due to the presence of gabbroic clots. SiO₂₍₁₀₎ shows a small but outside

1135 analytical error zigzag pattern. These variations reflect changes in the parental magma 1136 composition. 1137 1138 Figure 8. Temporal variation of La/Yb (based on ICPMS analyzes), CaO/TiO₂, Sr isotopes and 1139 Nb/Zr for Pu'u 'Ō'ō lava (see Figure 3 for color time periods). The trends for La/Yb and Sr 1140 isotopes are similar but inverse to each other. The CaO/TiO₂ trend is flat for most of the eruption 1141 except for the mixed and fractionated lavas (triangles) and some of the lava erupted late in the 1142 eruption (after day 10,000). The late lavas with high ratios probably have gabbroic clots with Fe-1143 Ti oxides. Nb/Zr shows and overall decrease during the eruption. 1144 1145 Figure 9. Plot of Th/Y vs. $K_2O_{(10)}$ and $CaO_{(10)}$, and Sr isotope ratios (see Figure 7 for the key to 1146 the colors). Note the overall good correlations of all of Th/Y with major elements and Sr isotopes 1147 for the unmixed Pu'u 'Ō'ō lava. The scatter of these trends indicates more than two sources are 1148 involved. The samples with anomalously low K₂O₍₁₀₎ and have CaO/TiO₂ of ≥4.70, which 1149 suggests the presence of gabbroic clots in the analyzed samples. 1150 Figure 10. Plot of ⁸⁷Sr/⁸⁶Sr ratios vs. SiO₂₍₁₀₎, CaO₍₁₀₎ and K₂O₍₁₀₎. The solid black line enclosed 1151 1152 samples erupted from 1992 to 2007 during Phase 3 and part of Phase 4. The colored fields are: 1153 blue, Phase 1; green, Phase 2; and orange, Phase 4 after 2007. A surge in magma supply 1154 occurred from 2003 to 2007. The good correlations of these geochemical parameters are 1155 consistent with a Mauna Loa-like source component that increased during this period.